ADDED MASS FORMULATION FOR FLUID-STRUCTURE INTERACTION

by

Afsoun Koushesh

A Thesis Presented to the Faculty of the
American University of Sharjah
College of Engineering
in Partial Fulfillment
of the Requirements
for the Degree of

Master of Science in
Mechanical Engineering

Sharjah, United Arab Emirates

May 2016

Approval Signatures

We, the undersigned, approve the Master's Thesis of Afsoun Koushesh.

Thesis Title: Added Mass Formulation For Fluid-Structure Interaction

Signature **Date of Signature** (dd/mm/yyyy)

_____ _____

Dr. Jin Hyuk Lee
Assistant Professor, Department of Mechanical Engineering
Thesis Advisor

_____ _____

Dr. Thomas Gally
Senior Lecturer, Department of Mechanical Engineering
Thesis Committee Member

_____ _____

Dr. Suheil Khoury
Professor, Department of Mathematics & Statistics
College of Arts and Sciences
Thesis Committee Member

_____ _____

Dr. Mamoun Fahed Saleh Abdel-Hafez
Head, Department of Mechanical Engineering

_____ _____

Dr. Mohamed El Tarhuni
Associate Dean, College of Engineering

_____ _____

Dr. Leland Blank
Dean, College of Engineering

_____ _____

Dr. Khaled Assaleh
Interim Vice Provost for Research and Graduate Studies

Acknowledgements

I would like to take this opportunity to express my appreciation to various people. I would like to thank to Dr. Jin Hyuk Lee, my advisor, for his guidance and precious suggestions throughout the past years at every single phase of my thesis progression. I also thank him for his kindness, understanding, patience, inspiration and extensive knowledge. My thanks also go to Dr. Mohamed El-Tarhuni, for his support during the summer registration period. I would also like to broaden my appreciation to MCE faculty members; Dr. Mamoun Abdel Hafez, Dr. Mohammad Gadallah, and Dr. Essam Wahba, for giving me the opportunity to receive a graduate teaching assistantship to continue my education at the American University of Sharjah. I am grateful to Dr. Thomas Gally and Dr. Suheil Khoury for their advice and help. I would also like to extend my sincere appreciation to Ms. Salwa Mohammed for her assistance. The completion of this work would not have been possible without my family and friends. I would like to thank them for their patience and understanding over the past few years. My genuine thanks go to my brother Ashkan Koushesh who provided me with all the emotional support and encouragement to complete this work.

Dedication

To my beloved
parents, and my
inspiring brother

For their love,
unconditional support
and encouragement

Abstract

Fluid-Structure Interaction (FSI) occurs due to interaction of multiple continuum fields. In our daily life, FSI is a common phenomenon. Birds flying in the air, leaves falling off the tree and waving flags are examples of the interaction of a structure with air. The forces of fluid (liquid/gas) that are acting on the structure will deform the adjacent elastic solid structure. The structural deformations are mainly enforced by fluid fields, acoustic fields and external forces. This work aims at demonstrating how variations of geometries' parameters would affect the fluid loading effect in water using COMSOL *Multiphysics 4.4* and compared with analytical data. Three-dimensional objects are placed in a water medium. A solid circular cylinder, a solid sphere, and a rectangular cantilever beam are placed in water and the acoustic wave is applied to the objects. More specifically, background acoustic pressure has been used to simulate an incident plane wave which excites the structures in water. Additionally, the inlet velocity and an outlet pressure are applied for fluid structure interaction investigation. When a structure is placed in water, the interaction between them plays an important role in determining the amount of fluid loading mass. The calculated results of added mass of the common geometry shapes match well with the analytical calculations and the discrepancy behavior of added mass amount due to the establishment of variation of geometries' parameters. More specifically, this research introduces an added mass effect study for fluid structure interaction while a specific micro electro mechanical system is submerged in water medium. Subsequently, based on the mentioned studies, an added mass formulation is derived for a specific MEMS (Micro Electro Mechanical System).

Search Terms: Fluid Structure Interaction, Added Mass, Common Geometry Shapes, Formulation, MEMS, Acoustics

Contents

List of Figures

List of Tables

List of Abbreviations

FSI	Fluid Structure Interaction
CFD	Computational Fluid Dynamics
MEMS	Micro Electro Mechanical System
FEA	Finite Element Analysis
FEM	Finite Element Method
AFM	Atomic Force Microscopy
OCSM	Optimizes Cubic Spline Method
LDV	Laser Doppler Vibrometer
FRA	Frequency Response Analyzer
DAQ	Data Acquisition

Chapter 1. Introduction

1.1. Overview

Fluid Structure Interaction (FSI) is the study of a structure that is surrounded by flowing and in some cases stationary fluid. FSI does have great relevance to numerous engineering applications, such as fluttering and buffeting of bridges, vibration of wind turbines, wind-plant contacts, aeroelastic response of airplane and several natural streams, such as blood flow in the vessels. When an object is moving in a fluid, the fluid surrounding the body will be displaced. The amount and direction of the displaced fluid are dependent on a number of criteria; for instance, the shape and orientation of the body, the amount of fluid surrounding the body, the type of the fluid and the external forces. The force required to accelerate the body immersed in fluid is much more than that needed in the case of air. The additional force will be needed in terms of added mass of the object in the fluid which will be added to the equation of motion. Finite Element Analysis (FEA) is a practical application of Finite Element Method (FEM) which is mostly used for studying the behavior of such coupling problems. Engineers and scientists are frequently using the FEM in order to model and solve the complex coupling multiphysics structure, mathematically and numerically respectively. The FEA application is also used to describe the Micro Electro Mechanical Systems (MEMS) behavior under water, which is the main focus of this study.

Micro Electro Mechanical System (MEMS) devices are trademark technology for the 21st century. Their ability to sense, analyze, compute and control all inside a single chip offers numerous innovative and influential products [1]. MEMS device is an up-and-coming device in a number of areas of science and technology, such as engineering structures, electronics, chemistry, physics, biology and health sciences. The two major key features of MEMS based devices are mechanical based structure to an electrical chip which gives a vast improvement to performance and functionality. These devices have been particularly used in the current marketplace for computer storage systems and automobiles due to the widespread use of sensors and actuators. Different kinds of sensors are used to sense the environmental conditions, and actuators are used to implement any action that is required to deal with the corresponding condition happening. Most MEMS devices are primarily based on

mechanical structures, such as beam, pump, gears and motors, as shown in Figure 1 [1].

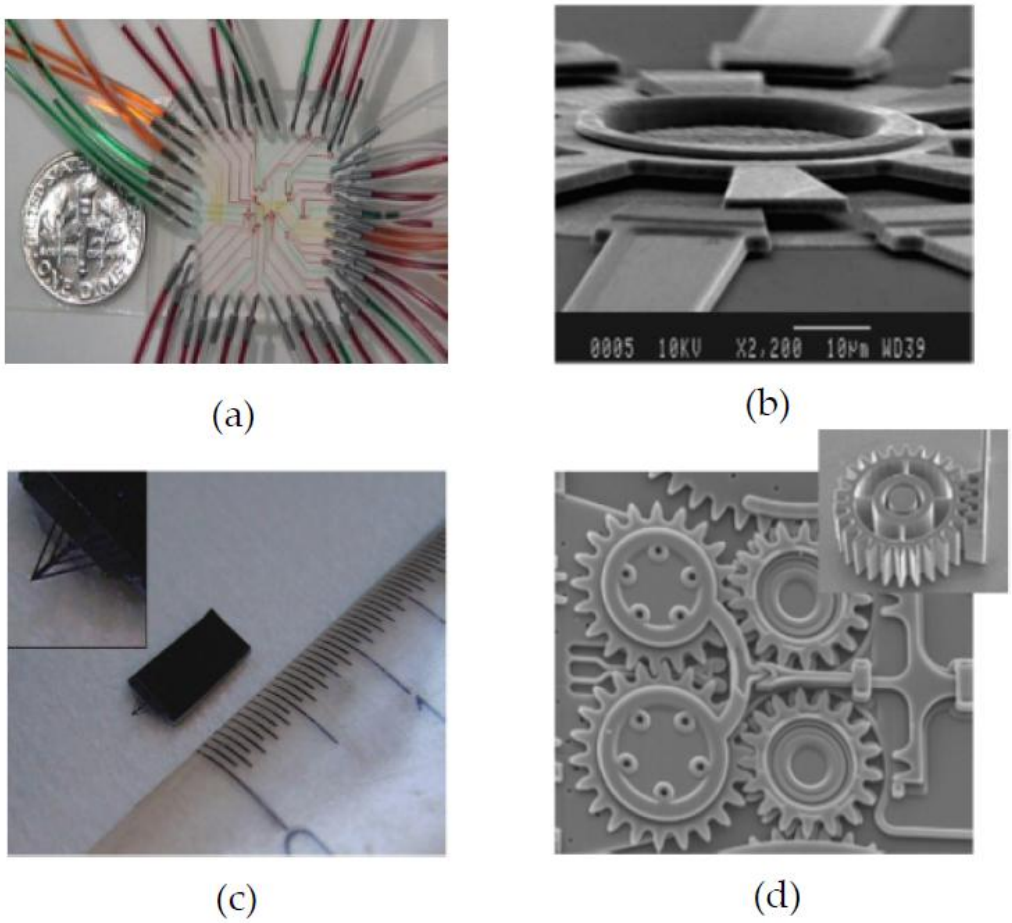

Figure 1: MEMS devices: (a) Micropump, (b) Micromotor, (c) Microbeam, (d) Microgear [1]

It has been stated that the simplest devices among MEMS are the beam based sensors in which they provide an extreme bright future for the evolution of new physical, chemical and biological sensors [1]. They are also verified to be multipurpose devices and are used in numerous fields, such as accelerometers and chemical sensors. MEMS beam based sensors mainly depend on the mechanical deformation of the beam. When the beam is burdened, the under stress elements will deform in which the structure shape changes and its corresponding static and dynamic behavior would be different than its unburdened case. The main idea behind the deflection comes from a load applied on the beam sides or along the surface. Normally, the loadings are either force applied on the structure or the added mass overwhelming/attached on the structure [1].

1.2. Objective

The primary objective of this study is to compute the hydrodynamic (added) mass of common geometry shapes, such as rectangular cantilever beam, solid sphere and circular cylinder. An extension of this objective is to determine the computed added mass with the variation of geometric parameters, so that such correlations may be used for designing sensor/transducers for underwater applications. In order to analyze how structures are experiencing the added mass loading effect differently by varying its geometry parameters, it is necessary to investigate the effect of each dimension of its geometry by comparing the numerical values of added mass. The following parametric study would be utilized to approximate the complicated geometry into a simple one. This methodology is used for determining the effect of added mass for the specific MEMS concerned in this study. This study might not be exact; however, it will at least provide a ballpark figure.

1.3. Thesis Report Organization

The current thesis is preceded with literature review on the added mass studies for the common geometry shapes and the MEMS in chapter 2. This is followed by the parametric study for the common geometry shapes and their corresponding added mass effects in chapter 3 and chapter 4, respectively. Furthermore, the added mass study for the specific beam based MEMS is presented in both mathematical and simulation based data in chapter 5. Chapter 6 concludes the presented study and suggests recommendations for future research.

Chapter 2. Literature Review

2.1. Common Geometry Shapes

Fluid Structure Interaction (FSI) occurs due to the interaction of multiple continuum fields. The added mass loading, also called hydrodynamic mass, is one of the most common FSI phenomenon. Basically, the added mass effect is when a structure acts as if it were heavier when it interacts with an external fluid continuum. Calculation of added mass has been widely studied in terms of deriving analytical formulas for the flexural and torsional resonant frequencies of common geometry shapes, such as cantilever beams, cylinders and spheres mostly. Various MEMS have been used in AFM for decades. Atomic force microscopy is a scanning probe with high resolution on order of a fraction of a nanometer [2]. Major efforts, both experimental and theoretical, have been done to study and understand the behavior of such elastic devices. Understanding the frequency behavior of such systems is dominant in the application to the atomic force microscope [3]. The frequency response of such elastic devices is highly reactive to the nature of the fluid in which they are immersed [2].

Sader et al. [4] used Elmer and Dreier's method to derive explicit analytical formulae for the numerical quantity of added mass, specifically for the rectangular cantilever beam. Sader et al. demonstrated a general hypothetical model for the frequency response of cantilever beam with an arbitrary cross sectional area. In this model, the cantilever beam is energized by a random driving force while immersed in a viscous fluid while assuming an arbitrary fluid density as well as the viscosity. The fundamental assumptions made toward the cantilever beam analysis are small vibration amplitude, incompressible fluid and the length of the beam must significantly exceed its width [4]. The general formulation is made based on specification of the hydrodynamic function that considered the cross section of the beam which was set to be a rectangular cross section. Depending on this study, the ratio between wet and dry natural frequencies is derived for different modes of vibration. The obtained formula can be used for obtaining the added mass effect on the rectangular cantilever beam. On the other hand, Liu et al. [5] propose an added mass matrix model based on dynamic responses of the beam when it is in contact with air and water where it can replicate any influence made by change in depth of water.

In this work, the real structure and the FEM models are used for validation of the proposed model as well as experimentation. There is an added mass correction factor proposed in Liu's [5] model, which compensates for the variation of the mass and stiffness matrices in real structure and the FEM analysis. One of the greatest improvements in this study is that this method could approximate the added mass matrix of water without consideration of any water related assumptions since all the water effects are represented in measured dynamic responses of the structure immersed in water.

Causin et al. [6] proposed a fluid structure model that simulates the propagation and encounters the added mass effect of incompressible fluid while a circular cylinder is immersed in water. In this model, a numerical and mathematical representation is proposed in order to clarify the coupled behavior of the cylinder immersed in water. The model represents the interaction between potential fluids coupling with linear elastic circular cylinder. This model has the capability to replicate the propagation phenomena; moreover, it accounts for the added mass effect of the fluid on the structure. More specifically, the fluid is presented by the Navier-Stokes equations in Arbitrary Lagrangian Eulerian formulation, and the cylinder at rest is described using a one-dimensional generalized string model [6]. Singhal et al. [7] derived an analytical model to describe the true and exact modes of vibration and corresponding natural frequencies of a circular cylinder and to find the added mass effect on the structure. The modal analysis was done through FEA, and the corresponding natural frequencies were obtained. The structure is described using the three-dimensional elastic theory, and the natural frequencies are derived through the well known energy method. Lastly, Singhal et al. [7] made an experimental setup to validate the model, and the obtained experimental data correspond to theoretical values. Lozzo et al. [8] studied the dynamic behavior of a circular cylinder submerged in water while the flexural oscillation was applied. The circular cylinder structure is idealized using one dimensional Euler Bernoulli beam and is immersed in water, where water is described through the potential theory. The sectional added mass corresponding to the inertial effects of hydrodynamic forces is firstly determined assuming cosine type deflected shape. Then, a lumped mass model is established, and the finite element method is devoted for finding the primary wet natural frequencies [8].

Govardhan et al. [9] focused on the study of the vorticities, forces and displacements to describe the dynamic behavior of the elastic sphere immersed in steady flow water. In their study, the behavior of sphere is described using the dynamics equation of the motion, considering the applied force on the structure by representing a phase angle between fluid force and body displacement. Using these equations, the natural frequencies for each mode are found in the case of vacuum. The corresponding wet natural frequencies are obtained through FEA analysis, and the added mass values are obtained for each mode. Experimentation was also performed to validate the obtained theoretical values. In another study of added mass for a sphere, Fackrell [10] developed a model in order to determine the forces acting on the sphere. He proposed two methods for dividing the total into unsteady drag and added mass components. The first approach relies on the linear form of equation that relates the added mass, dimensionless force, viscous drag and dimensionless displacement. The second method proposed is the Optimized Cubic Spline Method (OCSM) that uses cubic splines to estimate the added mass coefficient when a body is immersed in water. In Fackrell's study, the dynamic behavior of the sphere coupling with water is represented through elastic and potential theory, respectively. On the other hand, Ghassemi et al. [11] focused on calculating the added mass coefficient for the immersed sphere using numerical boundary element method. In their study, the fluid is assumed to be compressible and inviscid. Furthermore, the hydrodynamic forces and moments are determined by fluid inertia and the corresponding viscous properties due to the movement of immersed sphere. The method used in this study basically represents the hydrodynamic forces and the inertia as added mass terms. Kinetic energy of the fluid is described coupled with the dynamic behavior of the body along numerical methods such as Strip theory which could result in the added mass coefficient. Furthermore, the added mass coefficient obtained in this study has been validated along with the analytical value for the added mass. Moreover, the obtained added mass values were validated through experimentation.

2.2. Research Methodology

In this study, two hydrodynamics mass equations from White's work in [12] are used to estimate the analytical added mass value for each freely placed sphere and circular cylinder when the medium is accelerated at a certain rate. Moreover, the

equations of flexural and torsional resonant frequencies of a rectangular cantilever beam from Sader's et al. [4] study are used to evaluate the analytical amount of added mass when an incident plane wave excites both fluid and structure. The numerical added mass values of the structures obtained from both acoustic domain analysis and fluid domain analysis are compared to each other as well as with the analytical values. Finally, the obtained result shows how varying any of the geometries' parameters results in different added mass. In COMSOL *Multiphysics 4.4* module, the Acoustic module is used through a frequency domain analysis which will consequently lead to the study of added mass for a beam based MEMS.

Chapter 3. Added Mass Effect Parametric Study

3.1. Theory

A rectangular cantilever beam is one of the structures considered for this parametric study. Chu [13] represents the relationship of the natural frequency of a beam in different mediums in terms of fluid f_f and vacuum f_v. The script ρ is the density of fluid, ρ_c is density of the beam, and h and b are thickness and width of the beam, respectively. Equation 3.1 is valid for both viscid and inviscid stationary fluid model at macroscopic level.

$$f_f = f_v\left(1+\frac{\pi\rho b}{4\rho_c h}\right)^{-1/2} \tag{3.1}$$

A solid sphere and a circular cylinder are other geometries that are considered for this parametric study. In the following study, R is the radius of the sphere, and the symbols R and L are considered for the radius and the length of the circular cylinder respectively, while both are immersed in water with a density of ρ. The summation of forces on the system will be in terms of mass of the body and hydrodynamic mass (m_h). Based on the potential theory [8], the hydrodynamic mass depends on the shape of a body and the direction of the flow stream and can be calculated by summing the total kinetic energy of the fluid relating it to the kinetic energy of the body where dm is the mass element. In this context, the V_{rel} and U are velocity of the fluid associated with the body and velocity of fluid, respectively. Elgabaili [14] used the calculation of relative velocity (V_{rel}) as an approach for determining the added mass value when the body and fluid are moving at a certain velocity in which R is the radius, r is the radial direction, and θ is the azimuthal angle. However, in this parametric study, water is flowing at a certain velocity over the immersed structure. These equations are shown in Equations 3.2 - 3.5, where Equations 3.4 and 3.5 are the hydrodynamic mass of submerged sphere and cylinder, respectively.

$$KE_{fluid} = \int \frac{1}{2} V_{rel}^2 dm = \frac{1}{2} m_h U^2 \tag{3.2}$$

$$V_{rel}^2 = \frac{U^2}{4}\left(\frac{R}{r}\right)^6\left(1+3\cos^2\theta\right) \tag{3.3}$$

$$m_h = \frac{2}{3}\rho\pi R^3 \tag{3.4}$$

$$m_h = \rho\pi R^2 L \tag{3.5}$$

The 3D fluid structure interaction module in COMSOL *Multiphysics 4.4* is used through a frequency domain analysis and a transient analysis to demonstrate the added mass loading effect. The geometry shapes are all made of aluminum 3003-H18, and the dimensions for the given geometries are provided in Table 1. This parametric study is mainly done through varying any of the geometries' parameters that would result in added masses. In order to run the cantilever beam simulation, one of the parameters is varied while the other two parameters are kept fixed. This simulation is repeated until all the parameters are varied while one of the parameters is constant. For the case of a sphere, its radius was changing through a range of values to analyze its effect on the added mass value. Finally, for a circular cylinder, either the radius was kept and the length was varied or vice versa.

Table 1: Baseline Parameters of Geometry Shapes

Rectangular Cantilever beam		
Type	Symbol	Value
Width	*b*	0.1 m
Height	*a*	0.5 m
Length	*L*	4 m
Solid Circular cylinder		
Type	Symbol	Value
Radius	*R*	0.5 m
Length	*L*	4 m
Solid Sphere		
Type	Symbol	Value
Radius	*R*	0.5 m

In the pressure acoustic module, the acoustic wave is applied to the fluid medium which is water, immersing the geometries. More specifically, the background acoustic pressure field is used to generate a travelling plane wave which excites the structure in the water. Regarding the boundary conditions in the fluid structure interaction module, an inlet velocity of 1 *m/s* and an outlet pressure of 0 *kPa* are applied on the encountering water domain to study the fluid structure interaction, and the water domain outer faces are regarded as hard walls.

The rectangular cantilever beam structure is fixed at one end, and it is immersed in a rectangular water environment in both pressure Acoustics and Computational Fluid Dynamics (CFD) studies. On the other hand, for a sphere and a

circular cylinder, the water environment is modeled as a sphere and a box in pressure Acoustics and CFD studies, respectively and the geometries are freely spaced in these environments.

In fluid solid interaction module, all domains are meshed by Free Tetrahedral elements. Whereas, in the acoustic module, the computational mesh has to provide adequate resolution of the waves. In 3D acoustic models, it is essential to have a minimum of 6 elements per wavelength λ, and the maximum element size for mesh is the wavelength over 6, $L_{max}=\lambda/6=c/6f$, where c and f are the speed of sound and driving frequency, respectively. In the case of Acoustics module, both of global and sub models are solved in Eigen frequency and frequency domain. In the fluid structure interaction module, the model is solved using time dependent domain analysis.

Based on COMSOL simulations, the Eigen frequencies and kinetic energies are utilized to calculate the added mass in Acoustics and fluid structure interaction modules, respectively. Time harmonic analyses are performed under two different medium: water and air. The frequency responses obtained from the simulations, for the case of air, are represented in Figures 2 and 3. The similar plots were used for each parametric case, in two mediums, in order to find the wet (w_{wet}) and dry (w_{dry}) natural frequencies.

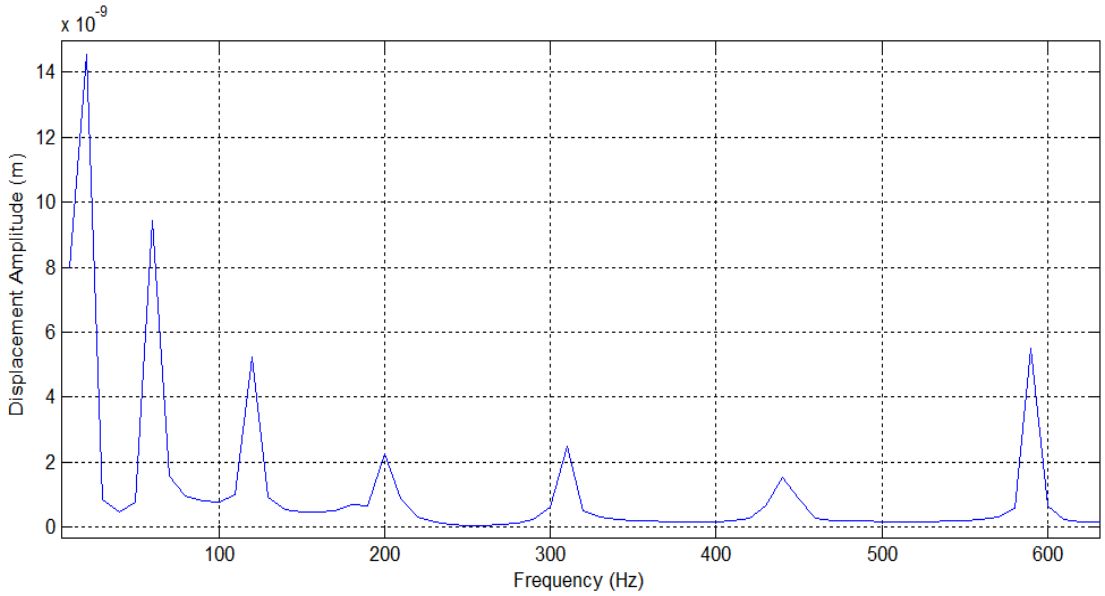

Figure 2: Frequency Response of Solid Sphere

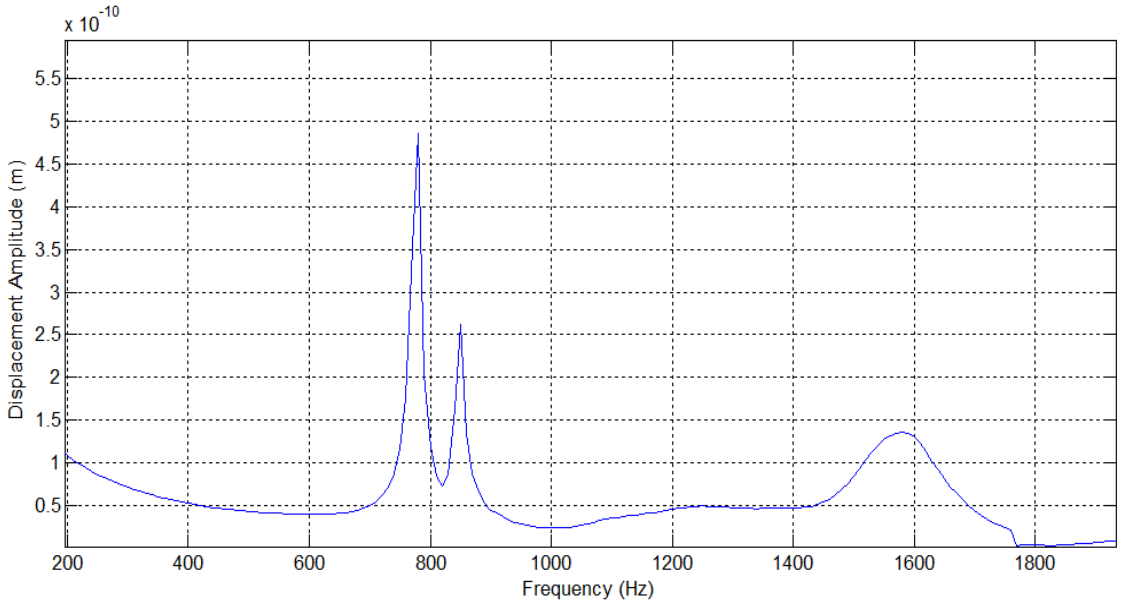

Figure 3: Frequency Response of Solid Circular Cylinder

In the case of fluid structure interaction, the average kinetic energy of the structure is obtained over one period of time using body surface integration. The calculated added mass of the common geometry shapes along with the analytical calculations, and the discrepancy behavior of added mass amount due to variation of geometries' parameters will be represented later in this text. Based on the obtained data, a percentage difference between the added mass values obtained from the two modules is calculated and is defined as "*E (%)* with CFD". In the COMSOL simulation, the total surface displacement result is represented for the geometry undergoing this parametric study.

3.1.1. Rectangular Cantilever Beam. The obtained numerical values of added mass for the cantilever beam using fluid structure interaction module are provided in Table 2 - 4. Based on White's [12] study, the integration of relative velocity to find the fluid kinetic energy (KE_{fluid}) can be obtained using body surface integration based on Equation 3.2.

$$m_h = 2\rho Lb(a+b) \tag{3.6}$$

Equation 3.6 from white's [13] study provides the hydrodynamic mass of a submerged cantilever beam where *a* and *b* are the height and the width of the beam.

Table 2: Fixed Length "L=4" using Kinetic Energy Method

Height a (m)	Width b (m)	Body Mass (Kg)	Added Mass (Kg)
0.5	0.1	546.00	542.68
0.6	0.2	1310.40	1401.34
0.7	0.3	2293.20	2270.51
0.8	0.4	3494.40	3440.19
0.9	0.5	4914.00	4789.53
1	0.6	6552.00	6497.11
0.4	0.7	3057.60	3009.24
0.3	0.8	2620.80	2600.15
0.2	0.9	1965.60	1901.79
0.1	1	1092.00	1030.57

Table 3: Fixed Height "a=0.5" using Kinetic Energy Method

Length L (m)	Width b (m)	Body Mass (Kg)	Added Mass (Kg)
4	0.1	546.00	542.68
3	0.2	819.00	950.96
2	0.3	819.00	809.79
1	0.4	546.00	542.53
5	0.5	3412.50	3398.87
6	0.6	4914.00	4876.25
7	0.7	6688.50	6592.95
8	0.8	8736.00	8688.19
9	0.9	11056.50	10997.58
10	1	13650.00	13255.37

Table 4: Fixed Width "b=0.1" using Kinetic Energy Method

Length L (m)	Height a (m)	Body Mass (Kg)	Added Mass (Kg)
4	0.5	546.00	542.68
3	0.4	327.60	321.84
2	0.3	163.80	171.51
1	0.2	54.60	53.45
5	0.1	136.50	223.18
6	0.6	982.80	966.68
7	0.7	1337.7	1333.92
8	0.8	1747.20	1736.35
9	0.9	2211.30	2188.86
10	1	2730.00	2692.15

According to the obtained data, as the cross section of the rectangular cantilever beam increases, the numerical value of added mass increases. When the

length is kept constant, the added mass value increases as the cross section increases in dimension, and it decreases while the cross section decreases. The obtained differences in percentage is relatively high, which indicates the need for further investigation on parametric analysis.

In the case of pressure Acoustics simulation, the wet and dry natural frequencies are obtained from the frequency plots. These natural frequencies are used in relation with what Sader et al. [4] suggested for the added mass. In order to find the natural frequency of the submerged cantilever beam, an incident plane wave is applied through a range of different frequencies in both air and water mediums, such as 10 Hz and 60 Hz as shown in Figures 4 and 5, respectively.

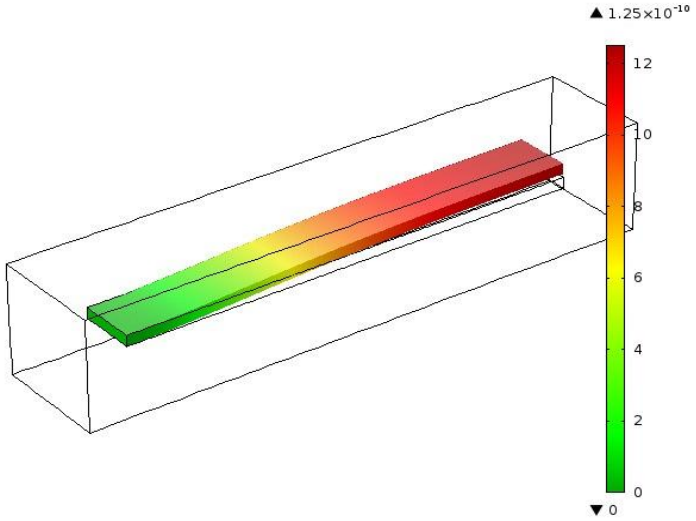

Figure 4: Surface Total Displacement in Frequency Domain of 10 [Hz]

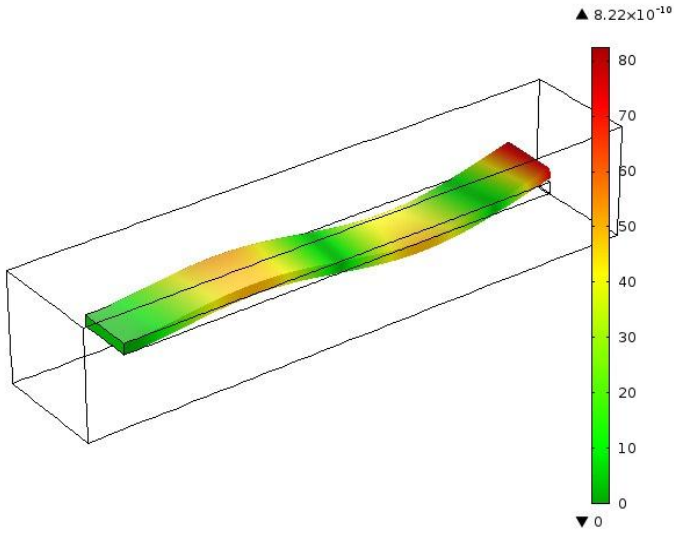

Figure 5: Surface Total Displacement in Frequency Domain of 60 [Hz]

The analytical equations used for acoustics calculations are provided in Equations 3.7 - 3.12, where the mass moment of inertia *I*, Young's modulus of elasticity *E*, cross sectional area *A* and dry natural frequency equations are used to find the added mass value.

$$\frac{f_f}{f_v} = \frac{W_{wet}}{W_{dry}} = N = \left(1 + \frac{\pi \rho b}{4 \rho_C h}\right)^{-1/2} \tag{3.7}$$

$$I = \frac{ab^3}{12} \tag{3.8}$$

$$W_{dry} = Cn^2 \sqrt{\frac{EI}{\rho A L^4}} \tag{3.9}$$

$$W_{wet} = N \cdot Cn^2 \sqrt{\frac{EI}{\rho A L^4}}$$

$$\rho_{added} = \frac{N^2 Cn^4 EI}{Wwet^2 AL^4} \tag{3.10}$$

$$m_{added} = \rho_{added} \cdot Vol \tag{3.11}$$

$$Vol = a \cdot b \cdot L \tag{3.12}$$

Consequently, calculations to find the added mass are done. On the other hand, the calculated added mass using pressure acoustic module is tabulated in Tables 5 - 7.

Table 5: Fixed Length "*L*=4" using Pressure Acoustics Module

Height *a* (m)	Width *b* (m)	W_wet (rad/s)	W_dry (rad/s)	Body Mass (Kg)	Added Mass (Kg)	*E(%)* with CFD
0.5	0.1	155.07	159.47	546.00	543.29	0.13
0.6	0.2	182.76	191.33	1310.40	1296.17	0.17
0.7	0.3	210.61	223.22	2293.20	2276.13	0.25
0.8	0.4	238.06	254.61	3494.40	3457.14	0.49
0.9	0.5	266.16	286.64	4914.00	4823.99	0.72
1	0.6	294.48	318.89	6552.00	6502.91	0.18
0.4	0.7	103.97	127.49	3057.60	3016.73	0.25
0.3	0.8	71.96	95.67	2620.80	2605.47	0.21
0.2	0.9	32.39	63.78	1965.60	1905.21	0.18
0.1	1	16.19	31.89	1092.00	1058.68	0.17

Table 6: Fixed Height "*a*=0.5" using Pressure Acoustics Module

Length *L* (m)	Width *b* (m)	W_wet (rad/s)	W_dry (rad/s)	Body Mass (Kg)	Added Mass (Kg)	*E(%)* with CFD
4	0.1	155.07	159.47	546.00	543.29	0.13
3	0.2	268.41	283.43	819.00	806.93	0.25
2	0.3	588.96	637.77	819.00	812.86	0.35
1	0.4	2300.17	2551.18	546.00	544.05	0.28
5	0.5	89.92	102.04	3412.50	3403.05	0.12
6	0.6	61.09	70.86	4914.00	4890.32	0.29
7	0.7	43.95	52.06	6688.50	6621.07	0.42
8	0.8	32.97	39.89	8736.00	8723.21	1.12
9	0.9	25.56	31.49	11056.50	11041.24	0.39
10	1	20.31	25.49	13650.00	13419.05	1.22

Table 7: Fixed Width "*b*=0.1" using Pressure Acoustics Module

Length *L* (m)	Height *a* (m)	W_wet (rad/s)	W_dry (rad/s)	Body Mass (Kg)	Added Mass (Kg)	*E(%)* with CFD
4	0.5	155.07	159.47	546.00	543.29	0.13
3	0.4	218.95	226.69	327.60	323.65	0.61
2	0.3	365.53	382.66	163.80	162.01	0.64
1	0.2	954.36	1020.69	54.60	54.02	1.05
5	0.1	17.98	20.41	136.50	136.14	0.25
6	0.6	83.07	85.04	982.80	969.01	0.24
7	0.7	71.42	72.78	1337.7	1334.19	0.76
8	0.8	62.61	63.73	1747.20	1738.44	0.12
9	0.9	55.81	56.69	2211.30	2191.29	0.11
10	1	50.29	51.01	2730.00	2697.66	0.21

In this case, as provided in the obtained data shown in Table 7, the wet natural frequencies are lower compared to the dry frequencies. Calculations are done to obtain the added mass values for each case. It is found that as the length is constant, the cross section and added mass values experience a direct relationship; whereas, when the constant parameter is height, a fluctuation occurs. This implies that the added mass increases as the cross section increases; nonetheless, at length of *1m* and width of *0.4m*, added mass value drops. After this combination of parameters, there is a direct relationship between the rectangular cross section and added mass. Finally, when the width is constant, there is also a direct relationship between the numerical value of cross section and added mass. Referring to the tables, the relative percentage error varies mainly as the length of the beam increases, and it increases the width of the beam. The percentage difference of the added mass obtained using acoustic

module and fluid structure interaction module is relatively low, which indicates that the modules will result close to each other.

3.1.2. Solid Circular Cylinder. The obtained added mass values for the solid circular cylinder, freely immersed in an inviscid water flow, using fluid structure interaction module are illustrated in Tables 8 - 9. Based on White's [12] study, the integration of relative velocity to find the fluid kinetic energy (KE_{fluid}) can be obtained using body surface integration. Accordingly, with the use of COMSOL Multiphysics, the kinetic energy of the structure that is obtained over one period of time (10 seconds) is averaged. The solid circular cylinder's total surface displacement for Fluid structure Interaction module at the first parametric sweep is shown in Figure 6.

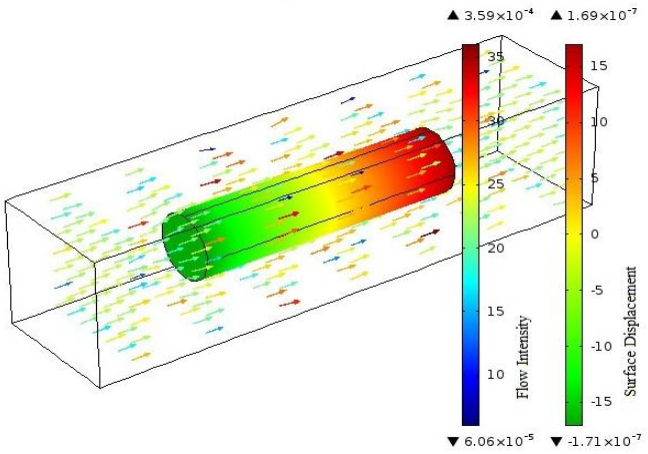

Figure 6: Surface Total Displacement in Fluid Structure Interaction Module

Table 8: Fixed Length "L=4" using Kinetic Energy Method

Radius R (m)	Body Mass (Kg)	Added Mass (Kg)
0.5	8576.55	3169.55
0.6	12350.23	4560.98
0.7	16810.03	6200.62
0.8	21955.96	8076.25
0.9	27788.02	10230.67
1	34306.19	12661.87
0.4	5488.99	2022.08
0.3	3087.56	1140.47
0.2	1372.25	503.91
0.1	343.06	126.02

Table 9: Fixed Radius "*R*=0.5" using Kinetic Energy Method

Length *L* (m)	Body Mass (Kg)	Added Mass (Kg)
4	8576.55	3169.55
5	10720.68	3948.19
6	12864.82	4743.48
7	15008.95	5524.72
8	17153.09	6327.79
9	19297.23	7108.16
10	21441.37	7912.09
3	6432.41	2365.14
2	4288.27	1585.24
1	2144.14	788.61

According to the data obtained for circular cylinder's parametric sweep, there is an increase in the added mass value as either radius or length increases. The low percentage difference between the analytical values shows the accurateness of the simulation.

The solid circular cylinder's total surface displacement for pressure acoustic module at the first parametric sweep is shown in Figure 7. In order to calculate the analytical acoustic added mass values, Equations 3.13 - 3.15 are used respectively. The obtained data is tabulated in Tables 10 and 11.

$$\frac{Wwet}{Wdry} = \frac{\sqrt{\frac{k}{mwet}}}{\sqrt{\frac{k}{mdry}}} = \frac{\frac{k}{mwet}}{\frac{k}{mdry}} = \frac{mdry}{mwet} \tag{3.13}$$

Step 1.

$$\frac{Wwet^2}{Wdry^2} = \frac{mdry}{mwet} \tag{3.14}$$

Step2.

$$AddedMass = mwet - mdry \tag{3.15}$$

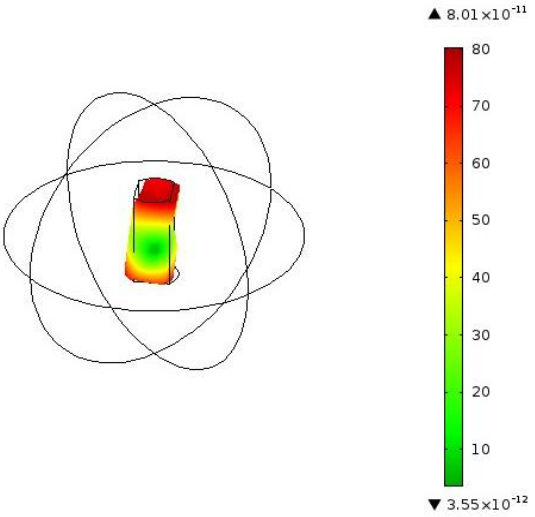

Figure 7: Surface Total Displacement in Pressure Acoustic Module

Table 10: Fixed Length "*L*=4" using Pressure Acoustic Module

Radius *R* (m)	W_wet (rad/s)	W_dry (rad/s)	Body Mass (Kg)	Added Mass (Kg)	*E(%)* with CFD
0.5	34.6	47.5	8576.55	3179.72	0.32
0.6	36.6	50.2	12350.23	4578.84	0.41
0.7	34.2	46.8	16810.03	6219.12	0.29
0.8	31.18	42.8	21955.96	8189.91	1.38
0.9	28.4	39	27788.02	10375.92	1.39
1	25.2	34.6	34306.19	12835.96	1.36
0.4	33.3	45.7	5488.99	2043.38	1.04
0.3	22.5	30.9	3087.56	1155.27	1.28
0.2	16.9	23.2	1372.25	513.94	1.95
0.1	7.8	10.7	343.06	127.68	1.31

Table 11: Fixed Radius "*R*=0.5" using Pressure Acoustic Module

Length *L* (m)	W_wet (rad/s)	W_dry (rad/s)	Body Mass (Kg)	Added Mass (Kg)	*E(%)* with CFD
4	34.6	47.4	8576.55	3172.82	0.11
5	24.6	33.6	10720.68	3926.78	0.54
6	16.2	22.3	12864.82	4784.16	0.85
7	12.5	17.2	15008.95	5621.55	1.72
8	10.1	13.9	17153.09	6412.12	1.32
9	8.3	11.4	19297.23	7161.72	0.75
10	4.9	6.8	21441.37	7989.85	0.97
3	44.3	60.9	6432.41	2406.74	1.73
2	58.6	80.4	4288.27	1597.95	0.79
1	72.8	100.1	2144.14	803.88	1.89

According to the data obtained using acoustic module, there is also an increase in the added mass value as either radius or length increases, which is similar to what is obtained in the CFD analysis. The low percentage difference between the CFD values shows the accuracy of both modules.

3.1.3. Solid Sphere. The obtained added mass values for the solid sphere, freely immersed in an inviscid water flow, using fluid structure interaction module are illustrated in Table 12. Based on White's [13] study, the integration of relative velocity to find the fluid kinetic energy (KE_{fluid}) can be obtained using body surface integration. Accordingly, with the use of COMSOL Multiphysics 4.4, the kinetic energy of the structure that is obtained over one period of time (10 seconds) is averaged. The solid circular cylinder's total surface displacement for Fluid structure Interaction module at the first parametric sweep is shown in Figure 8.

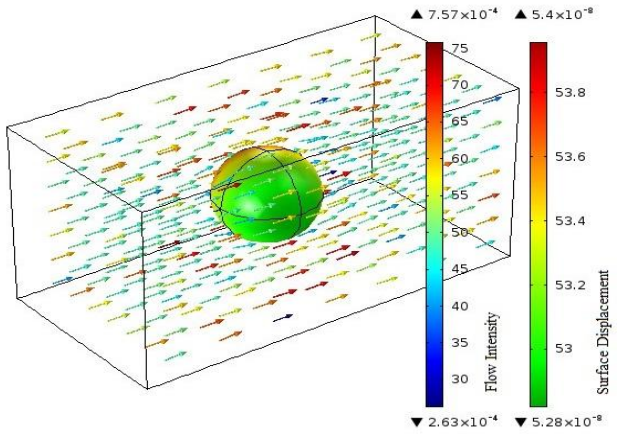

Figure 8: Surface Total Displacement in Fluid Structure Interaction Module

Table 12: Varying Radius "*R*" using Kinetic Energy Method

Radius *R* (m)	Body Mass (Kg)	Added Mass (Kg)
0.5	1429.42	263.38
0.6	2470.04	456.23
0.7	3922.34	721.75
0.8	5854.92	1078.22
0.9	8336.40	1528.64
1	11435.39	2102.35
0.4	731.86	135.26
0.3	308.75	56.68
0.2	91.48	16.88
0.1	11.44	2.09

According to the data obtained for solid sphere's parametric sweep, there is an increase in the added mass value as either radius or length increases. The low percentage difference between the analytical values shows the accurateness of the simulation.

The solid sphere's total surface displacement for pressure acoustic module at the first parametric sweep is shown in Figure 9. In order to calculate the analytical acoustic added mass values, Equations 3.13 - 3.15 are used respectively, and the obtained data is tabulated in Table 13.

$$\frac{Wwet}{Wdry} = \frac{\sqrt{\frac{k}{mwet}}}{\sqrt{\frac{k}{mdry}}} = \frac{\frac{k}{mwet}}{\frac{k}{mdry}} = \frac{mdry}{mwet} \tag{3.13}$$

Step 1.

$$\frac{Wwet^2}{Wdry^2} = \frac{mdry}{mwet} \tag{3.14}$$

Step2.

$$AddedMass = mwet - mdry \tag{3.15}$$

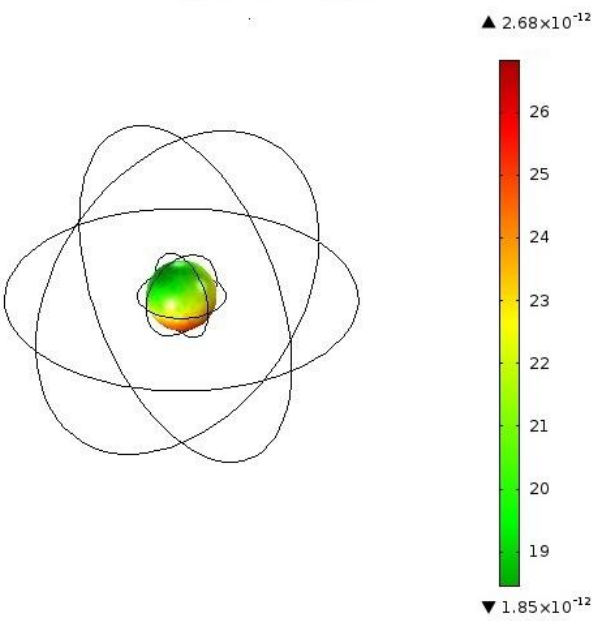

Figure 9: Surface Total Displacement in Pressure Acoustic Module

Table 13: Varying Radius "*R*" using Pressure Acoustics Module

Radius *R* (m)	W_wet (rad/s)	W_dry (rad/s)	Body Mass (Kg)	Added Mass (Kg)	*E(%)* with CFD
0.5	37.5	75.7	1429.42	266.72	1.25
0.6	46.4	74.8	2470.04	461.53	1.15
0.7	23.4	40.1	3922.34	730.27	1.17
0.8	20.2	36.8	5854.92	1100.81	2.05
0.9	19.3	36.2	8336.40	1550.85	1.43
1	10.1	20.5	11435.39	2145.92	2.03
0.4	104.1	106.3	731.86	138.18	2.11
0.3	112.5	118.7	308.75	57.61	1.61
0.2	115.2	122.4	91.48	17.32	2.54
0.1	100.4	107.5	11.44	2.12	1.42

The obtained data shown in Table 13 reveals that the wet natural frequencies are lower compared to the dry frequencies. The results indicate that the added mass increases when the radius is increased. This outcome is similar to the result obtained through CFD analysis. Nonetheless, this low percentage difference between the acoustic and fluid structure interaction analysis shows the closeness of the modules for the same case study.

Chapter 4. Added Mass Effect for a Special MEMS

The MEMS structure that has been selected for this study is shown in Figure 10, in which two identical beams are connected by a torsional spring in the middle. In Figure 10, *F* is the excitation force, *#1* and *#2* are used for numbering each beam, *C* is the damping coefficient of dampers, *K* is the spring and torsional stiffness and *L* represents the beam length. Both beams have rectangular cross sections. As shown in the figure, both free ends of each beam are connected to a spring and a damper that are fixed to the ground. There is a harmonic excitation force applied at the free tip of beam *#2* which will end up having a forced damped coupling vibration. The vibrational behavior of the following 2 degree of freedom system has been studied through hand calculations. Consequently, the plot response of the system due to a harmonic wave has been obtained using MATLAB software. The codes for this part are provided in the Appendix A. In other words, the analytical values of natural frequencies are compared to the natural frequencies obtained from coupled transfer function plot of the selected MEMS. It is worth noting that the structure is symmetrical in all terms; this indicates that the beams have the same length, same cross sectional area and same body mass (m_1 equals to m_2). In addition, the damping values of C_1 and C_2 are equal and also the spring stiffness values of K_1 and K_2 are equivalent.

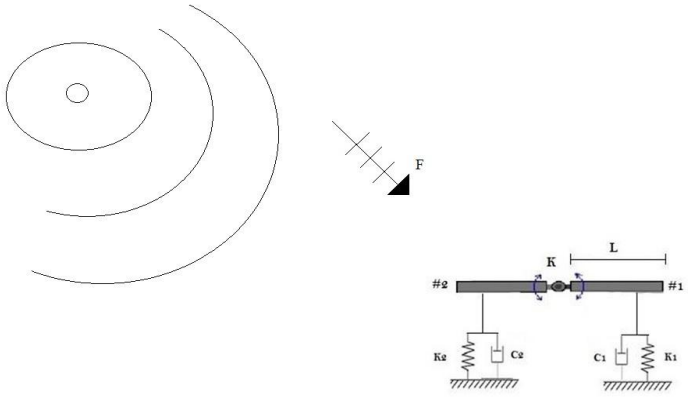

Figure 10: Selected MEMS

The main objective of this thesis is to study the behavior of this forced vibrating system when submerged in water. It is a challenge to consider the effect of

surrounding water on the behavior of the structure extensively. The general effect of surrounding fluid on any structure is mainly adding extra mass which causes distortion in both flow and the behavior of the structure. More specifically, the surrounding water will add extra mass to the mass of beam itself, extra damping to each *C* and extra stiffness to each *K*. In this fluid structure interaction study, water is assumed to be a still fluid which will be excited due to the vibrational motion of the structure. Referring to literature, when the flow behavior is changed drastically due to structural vibration and high amplitude, which cannot be neglected, the system is called strongly coupled fluid structure interaction system [15]. In contrast, weakly coupled fluid structure interaction happens when the flow behavior is changed slightly [15]. Accordingly, in the current study, the weakly coupled system is studied in terms of added mass, stiffness and damping to the system. However, the main focus is on formulating the added mass effect for this specific system. The added effects due to presence of fluid medium are dependent on several factors such as structure cross section shape, the Reynolds number, surface roughness, flow velocity, motion of the structure, etc. [16]. It is been stated that there is no such solution or model that can consider all the factors simultaneously [16]. The 2 degrees of freedom behavior of the selected MEMS, when it stands by no external medium, are represented in Equations 4.1 and 4.2 that represent the equation of motion for beam *#1* and *#2*, respectively. Where θ_1 and θ_2 are the generalized coordinates, $e^{i\omega t}$ is the applied harmonic force. These equations are derived using Newton's Second Law and Euler Law based on the Free Body Diagram of the selected MEMS shown in Figure 11.

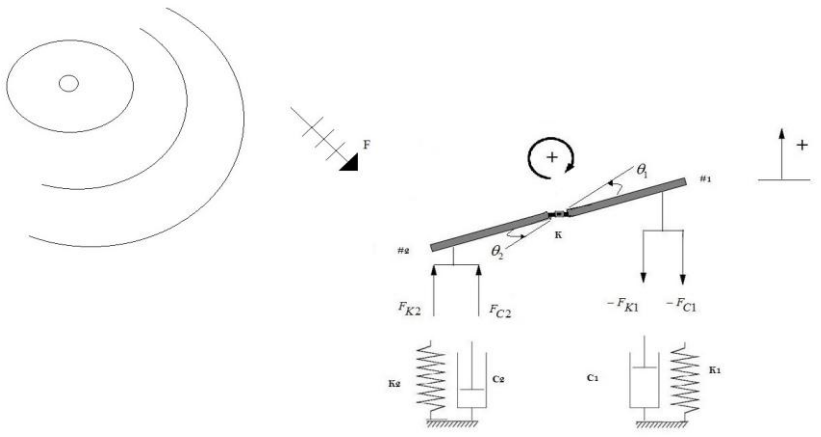

Figure 11: Free Body Diagram

$$m_1 L\ddot{\theta}_1 + \dot{\theta}_1(-C_1L - C_2L) + \dot{\theta}_2(C_2L) + \theta_1(KL - K_1L + K_2L) + \theta_2(K_2L - KL) = e^{i\omega t} \quad (4.1)$$

$$m_2 L\ddot{\theta}_2 + \dot{\theta}_1(C_2L) + \dot{\theta}_2(-C_2L) + \theta_1(K_2L - KL) + \theta_2(KL - K_2L) = e^{i\omega t} \quad (4.2)$$

General equation of motion of this MEMS in matrix form is

$$[M_S]\cdot\{\ddot{\theta}\} + [C_S]\cdot\{\dot{\theta}\} + [K_S]\cdot\{\theta\} = [F] \quad (4.3)$$

where M_s is the mass matrix of the MEMS, C_s is the damping of the structure, K_s is the spring and torsional stiffness attached to the MEMS, and F is the harmonic acoustic wave force applied on the MEMS.

In this stage, the fluid loading effects on the MEMS are considered in each equation of motion. The additional terms such as the added mass m_a, added damping coefficient C_a and added spring stiffness K_a show the effect of added water represented in Equations 4.4 and 4.5. These effects added due to presence of fluid medium are all unique for each different fluid [17]. Sedlar [17] suggests that the additional water stiffness effect for most of the common structures such as beams are neglected which means that all the K_a terms will be set equal to zero in the equations. Hence, the remaining damping and mass effect of water is studied in the coming sections.

$$(m_1 + m_{1a})L\ddot{\theta}_1 + L\dot{\theta}_1(-(C_1 + C_{1a}) - (C_2 + C_{2a})) + L\dot{\theta}_2((C_2 + C_{2a})) + L\theta_1((K + K_a) - (K_1 + K_{1a}) + (K_2 + K_{2a})) + L\theta_2((K_2 + K_{2a}) - (K + K_a)) = e^{i\omega t} \quad (4.4)$$

$$(m_1 + m_{1a})L\ddot{\theta}_1 + L\dot{\theta}_1(-(C_1 + C_{1a}) - (C_2 + C_{2a})) + L\dot{\theta}_2(C_2 + C_{2a}) + L\theta_1(K - K_1 + K_2) + L\theta_2(K_2 - K) = e^{i\omega t}$$

$$(m_2 + m_{2a})L\ddot{\theta}_2 + L\dot{\theta}_1(C_2 + C_{2a}) + L\dot{\theta}_2(-(C_2 + C_{2a})) + L\theta_1((K_2 + K_{2a}) - (K + K_a)) + L\theta_2((K + K_a) - (K_2 + K_{2a})) = e^{i\omega t} \quad (4.5)$$

$$(m_2 + m_{2a})L\ddot{\theta}_2 + L\dot{\theta}_1(C_2 + C_{2a}) - L\dot{\theta}_2(C_2 + C_{2a}) + L\theta_1(K_2 - K) + L\theta_2(K - K_2) = e^{i\omega t}$$

4.1. Added Mass Study

4.1.1. Assumptions. To start the added mass study, a number of assumptions that have been implemented on developing the MEMS model and its corresponding calculations should be noted. These assumptions are as follows:

- Symmetric MEMS
- Fluid is considered to be inviscid, stationary and adiabatic
- No internal damping
- The fluid is compressible
- Vortex made due to added fluid is neglected
- Spring and dampers are assumed to be ideal elements
- Torsional spring is assumed to be an ideal element
- Uniform cross section over the entire beam length
- Beams are made of linear elastic isotropic material
- Internal frictions of beams are neglected
- The selected fluid is water
- Beams are made of Aluminum H3003-18
- Vibration amplitude of the beams is assumed to be very small compared to their length scale

4.1.2. Simulation. As stated earlier in this report, the submerged structure experiences extra added mass, which affects the dynamic behavior of the structure. The two second order ordinary differential sets of equation of motions are arranged in a matrix form in order to find the eigenvalues and the natural frequencies. This process is done using MATLAB software. Firstly, the structure behavior is studied with no extra medium than air, and the analytical natural frequencies are compared with the transfer functions obtained from the equation of motions of coupled structure. Secondly, a symbolic study is done for two cases of air and water medium. For the ease of representation, as stated earlier, 'dry' is the term used for the case of air surrounding the structure while 'wet' is used when water is provided around the structure. The first two natural frequencies are obtained in both dry and wet cases, symbolically. The MATLAB code is provided in Appendix B in which $m_1 = m_2 = m$,

$K_1 = K_2$, and $C_1 = C_2 = C$, and added mass is represented by m_a. In order to find the relation between wet and dry natural frequencies, ratios R_1 and R_2 are defined for the first and second natural frequencies as shown in Equations 4.6 and 4.7, respectively.

$$R_1 = \frac{\omega_{1wet}}{\omega_{1dry}} \tag{4.6}$$

$$R_2 = \frac{\omega_{2wet}}{\omega_{2dry}} \tag{4.7}$$

In the above equations ω_{1wet} and ω_{2wet} are the first two natural frequencies when water is added to the structure, and ω_{1dry}, ω_{2dry} are the first and second natural frequencies when there is air around the structure only.

The baseline parameters for the Symmetric MEMS that are used for the numerical investigations are provided in Table 14.

Table 14: Baseline Parameters for the MEMS

Micro Electro Mechanical System		
Type	Symbol	Value
Width	b	1×10^{-6} m
Thickness	t	0.05×10^{-6} m
Length	L	1×10^{-6} m
Spring Stiffness	$K_1 = K_2$	20×10^{-6} N/m
Torsional Spring Stiffness	K	1000×10^{-6} N/m
Damping Values	$C_1 = C_2 = C$	0 N.s/m
Beam Mass	$m_1 = m_2 = \rho_{Al} \cdot t \cdot b \cdot L$	1.365×10^{-31} g
Fluid Density	ρ_f	1000 kg/m^3
Aluminum H3003-18 Density	ρ_{Al}	2730 kg/m^3
Modulus of Elasticity of Aluminum	E	70 Gpa
Modulus of Elasticity of Polysilicon	E	160 Gpa

In this stage, the COMSOL *Multiphysics 4.4* is used for the added mass study in which the identical system with the same baseline parameters is designed in the Acoustic module where the outer box resembles the environment around the MEMS and the simulation is computed for two cases. These cases are when the encountered box is once made of air and the corresponding dry frequencies are obtained. The second case is when the outer box is set to be a water domain and the obtained natural frequencies are corresponding to the wet case. Therefore, the first and second natural frequencies in both cases are determined. It is worth noting that the cylinder attached in between the beams is modeled to resemble the torsional spring and its corresponding stiffness is added. The first two natural frequencies for the dry case are then compared with the simulated results using MATLAB codes. The obtained frequencies are deviating from each other by 12 % for the first natural frequency and 9.5% for the second natural frequency variation which is reasonable due to the different numerical computing methods they are made of and operating at. The MEMS structure is modeled as shown in Figure 12, where the attached thin plates are modeled in order to resemble the spring and damper as of that attached to the MEMS at the tip of each beam. These thin vertical plates are chosen to be made of Polysilicon, and the values of the spring and dampers are added to them according to the baseline parameters defined earlier.

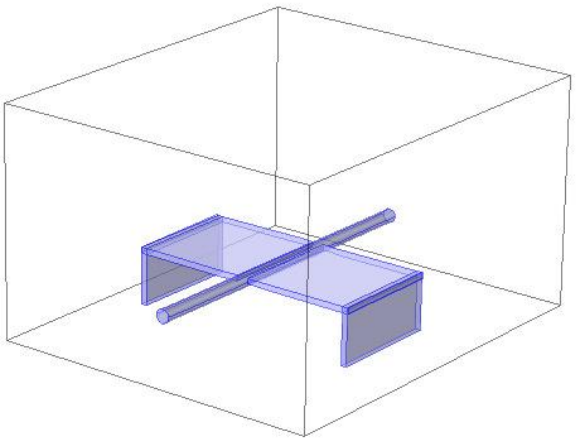

Figure 12: MEMS Modeled in Acoustic Module in COMSOL

The first and second mode shapes corresponding to natural frequencies are obtained for the MEMS placed in both air and water mediums. The frequency response of the MEMS placed in air is represented in Figure 13, and its corresponding eigenmode shape is represented in Figure 14. Similarly, the frequency response of the MEMS submerged in water is represented in Figure 15, and its corresponding eigenmode shape is represented in Figure 16.

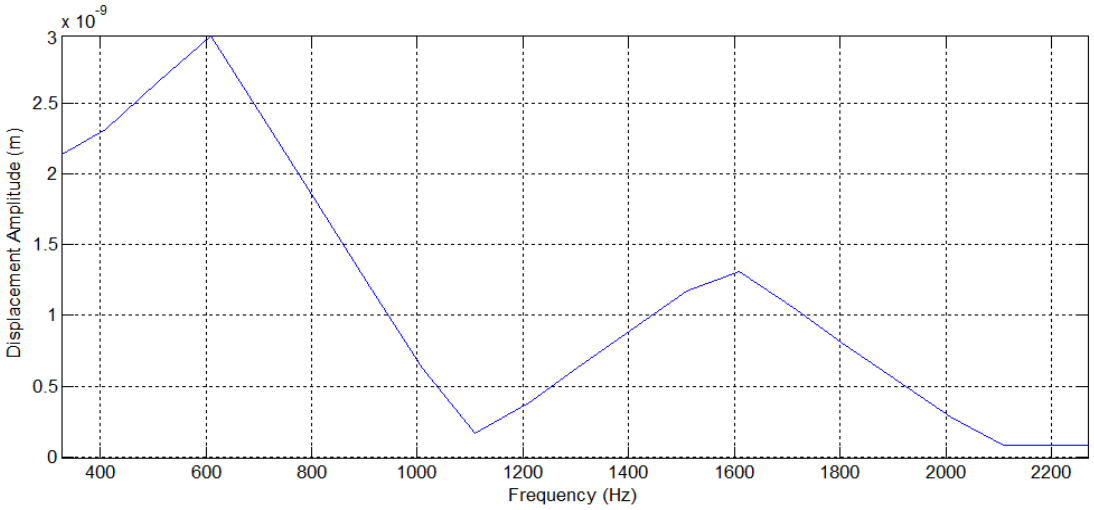

Figure 13: Frequency Response of MEMS in Contact with Air

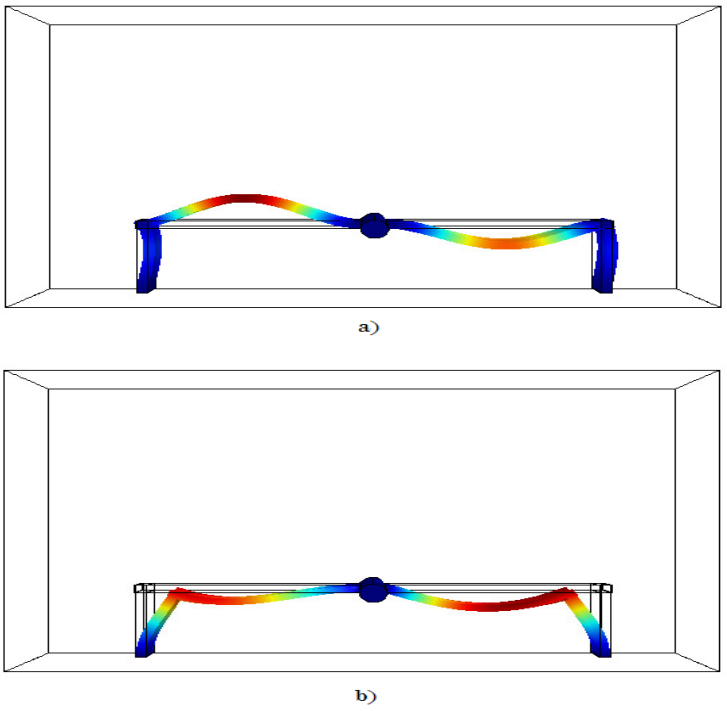

Figure 14: (a) First Eigenmode (Rocking) (b) Second Eigenmode (Bending) Shapes of the MEMS in Air (yz Plane View)

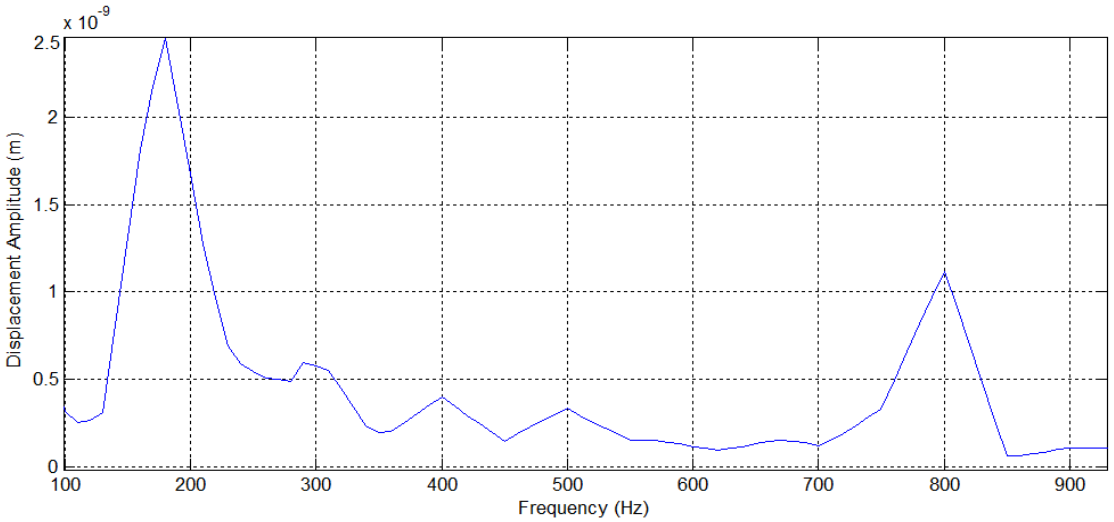

Figure 15: Frequency Response of the MEMS Submerged in Water

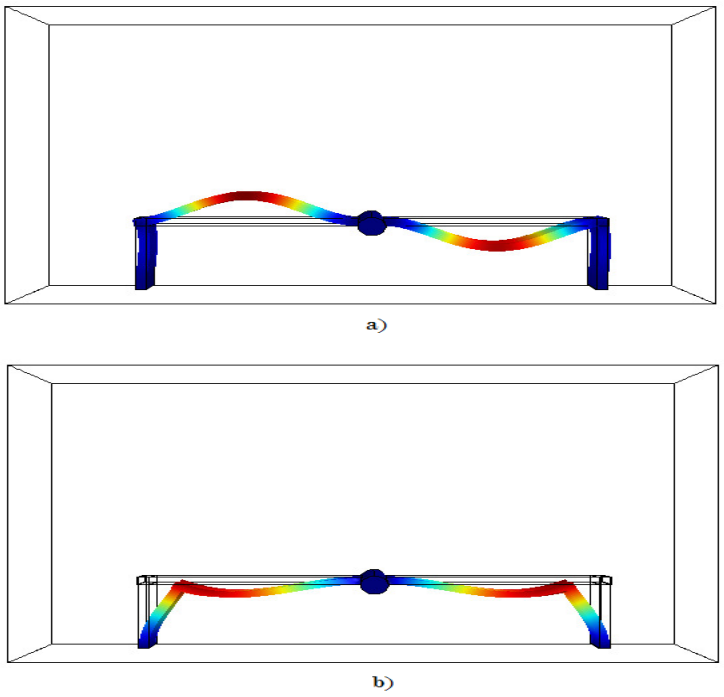

Figure 16: (a) First Eigenmode (Rocking) (b) Second Eigenmode (Bending) Shapes of the MEMS in Water (yz Plane View)

At this point, where the natural frequencies obtained from MATLAB and COMSOL *Multiphysics 4.4* are well matched, this data can be used in the suggested formulas in order to find the effect of added mass on the selected MEMS. In the following parts, the two suggested formulas based on Acoustic and elastic beam theory are explained in detail, and the corresponding added masses are calculated,

respectively. The eigenmode shapes and their corresponding natural frequencies for the first two modes of the MEMS are presented in Table 15, where subscript *i* stands for the eigenmode number, $\omega_i Wet$ and $\omega_i Dry$ represent the natural frequencies in water and air cases, respectively.

Table 15: Eigenmode Numbers and Corresponding Natural Frequencies

Micro Electro Mechanical System		
Mode	Natural Frequency in air	Natural Frequency in water
i	$\omega_i Dry$ (Hz)	$\omega_i Wet$ (Hz)
1	660	175
2	1630	800

Moreover, these obtained natural frequencies are used for calculating the added mass values through different methods. Then, these obtained added mass values are compared to the added mass obtained using general ratio of dry and wet natural frequencies in Equations 4.6 and 4.7.

4.1.3. Acoustics Method. In this section, acoustic wave propagation in fluid is considered for providing an added mass equation for the specific selected MEMS. The fluid can be either liquid or gas while in this study the goal is to study the liquid effect on the structure. The fluid flow is assumed to be macroscopic, which means that the fluid properties resemble the summation of all the molecular properties. Acoustic waves are microscopic oscillations of pressure that are directly linked with the local motion of fluid particles. This is the reason behind mainly using differential equations of acoustic pressure for modeling the fluid coupling with a structure [18]. In the case of fluid structure coupling interaction, the behavior of fluid pressure could be expressed by Helmholtz's equation below which is an acoustic wave equation:

$$\frac{1}{c^2}\frac{\partial^2 \mathrm{P}}{\partial t^2} - \nabla^2 \mathrm{P} = 0 \tag{4.8}$$

This equation is derived based on Navier-Stokes equation of motion and continuity equation, where *P* is the fluid's pressure, *c* is the speed of sound in fluid medium, ∇^2 is the Laplacian operator, and *t* stands for time [19]. The Laplacian

operator in Helmholtz's equation can be described by introducing it in terms of Laplacian matrix notation:

$$\frac{1}{c^2}\frac{\partial^2 \mathrm{P}}{\partial t^2} - \{L\}^T \cdot (\{L\}\mathrm{P}) = 0 \tag{4.9}$$

Galerkin procedure [20] is used for discretization of Equation 4.9 and is then multiplied by a virtual pressure change defined as $\delta P = \delta P(x, y, z, t)$ where the *x, y, z, t* are the pressure changes in each direction with respect to time [19]. Discretized equation is then integrated over the volume of the domain and is equated to the integration over surface in which the derivative of pressure normal to the surface is enforced which is shown in Equation 4.10. [21].

$$\int_v \frac{1}{c^2}\delta P \frac{\partial^2 \mathrm{P}}{\partial t^2} dv + \int_v (\{L\}^T \delta P) \cdot (\{L\}\mathrm{P}) dv = \int_S \{n\}^T \delta P (\{L\}\mathrm{P}) dS \tag{4.10}$$

In the above equation, *v* represents the volume of domain and *{n}* is the unit normal to the interface *S*.

Continuity equation is used for deriving the interaction between the fluid and structure at the interface boundary. The normal displacement of the structure has to be equal to the normal displacement of the fluid. Hence, the fluid momentum equation is described at the fluid structure interface *S* in terms of normal pressure gradient of the fluid and normal acceleration of the structure [21].

$$\{n\} \cdot \{\nabla P\} = -\rho_0 \{n\} \cdot \frac{\partial^2 U}{\partial t^2} \tag{4.11}$$

In the above equation, ρ_0 is the fluid density and *U* is the displacement vector of the structure at the interface *S*.

Assuming a rigid wall boundary will make the right side of Equation 4.11 equal to zero. This assumption is mainly the no slip condition where fluid velocity is identical to the surface velocity is:

$$\{n\} \cdot \{\nabla P\} = 0 \tag{4.12}$$

The applied force matrix *[F]* is an acoustic sound plane wave radiation applied on the coupling structure which is shown in Equation 4.13.

$$[F] = p_0 e^{i\vec{k}\cdot\vec{r}} \tag{4.13}$$

Where p_0 is the pressure amplitude of wave radiation, propagation vector is described as $\vec{k} = \vec{i}k_X + \vec{j}k_Y + \vec{\kappa}k_Z$, and the vector position is defined as $\vec{r} = \vec{i}_x + \vec{j}_y + \vec{\kappa}_z$. In the mentioned equation k_x, k_y, and k_z are complex constants describing wave number vector k. More specifically, a time harmonic mean of is considered $e^{j\omega t}$. The script ω stands for the angular frequency of the applied plane wave which is related to frequency $\omega=2\pi f$. The wave number k is defined as the ratio ω/c which shows the relation between angular frequency and speed of sound. Referring back to Figures 13 and 14, the first two eigenmode shapes for both mediums, only small changes in eigenmode shapes between air and water mediums are detected. The study of eigenmodes is cautiously studied and strongly established in preceding works such as Liang et al. [22] and Meirovitch's [23] in which it is proven that the eigenmodes in air and water are almost identical. Since the mode shapes are validated to be the same in the two mediums, the maximum potential energy remains constant in these two mediums. Similarly, the kinetic energy of the vibrating MEMS will also remain unchanged [19]. When the MEMS is vibrating in the water medium, part of its kinetic energy will be lost while struggling to enhance the kinetic energy of the surrounding water through implementing work in opposition to the force of water. As a result the velocity of the vibrating MEMS will decay and thus the natural frequencies will also experience a decrease [23]. Accordingly, the relation between natural frequencies in the two mediums can be expressed as shown in Equations 4.14 and 4.15 below:

$$\omega_{dry}^2 = \left(\frac{P_s}{K_s}\right)_{air} \tag{4.14}$$

$$\omega_{wet}^2 = \left(\frac{P_s}{K_s + K_F}\right)_{water} \tag{4.15}$$

In the above equations, P_s is the maximum potential energy of the structure, K_s and K_F are initial kinetic energy of the structure and fluid respectively. Defining a ratio between the kinetic energies as λ in Equation 4.16 will provide the relation between the natural frequencies obtained as shown in Equation 4.17.

$$\lambda = \frac{K_F}{K_s} \tag{4.16}$$

$$\frac{\omega_{wet}}{\omega_{dry}} = \frac{1}{\sqrt{1+\lambda}} \tag{4.17}$$

The kinetic energies could be interpreted in terms of mass as shown in Equations 4.18 and 4.19 below:

$$K_s = M_s \cdot \int_v W^2(x,y,z) \cdot dv \tag{4.18}$$

$$K_F = M_a \cdot \int_v W^2(x,y,z) \cdot dv \tag{4.19}$$

where M_s is the mass of MEMS, M_a is the added mass due to fluid presence, v represents the volume of the MEMS, and $W(x,y,z)$ describes a function in terms of three dimensional displacement.

Therefore, the ratio defined in Equation 4.16 becomes [23]

$$\lambda = \frac{M_a}{M_s} \tag{4.20}$$

Now, combining Equation 4.17 with Equation 4.20 and solving simultaneously for M_a would result in

$$M_a = \left(\frac{\omega_{dry}^2 - \omega_{wet}^2}{\omega_{dry}^2} \right) \cdot M_s \tag{4.21}$$

The obtained natural frequencies represented earlier in Table 15 are used in Equation 4.21 above in order to calculate the added mass M_a for each mode shape i. The obtained added mass values are tabulated in Table 16 below. According to [24], the obtained values indicate that the added mass values of the lower modes are higher compared to the higher modes.

Table 16: Added Mass Values Through Acoustic Method

Acoustic Method for the MEMS	
Mode	Added Mass (g)
i	M_{ia}
1	2.538×10^{-31}
2	2.072×10^{-31}

4.1.4. Beam Theory. In this section, vibration energy of the beam is studied for investigation of the added mass for the selected MEMS. Vibration energy is presented as a summation of kinetic and potential energies of the selected Micro Electro Mechanical System. As a harmonic vibration is applied, the displacement of the beam is given by *y(x,t)*

$$y(x,t) = A_i \varphi_i e^{\omega \cdot t} \tag{4.22}$$

where A is the amplitude, ω is the frequency at which the beam oscillates, φ is the eigenmode shape, and the subscript i is the mode number [25].

The general equations for the kinetic and potential energies are represented in Equations 4.23 and 4.24. Where *PE* is a notation for potential energy, *KE* represents the kinetic energy, D is the flexural rigidity of the beam, L is the length of the beam, and the script m represents the mass of the beam.

$$PE = \frac{1}{2}\int_0^L D \cdot \left[\frac{\partial^2 y(x,t)}{\partial x^2}\right]^2 dx \tag{4.23}$$

$$KE = \frac{1}{2}\int_0^L m \cdot \left[\frac{\partial y(x,t)}{\partial t}\right]^2 dx \tag{4.24}$$

In the case where the water medium is added, the beam experiences an additional mass term in the kinetic energy equation. Accordingly, the applied pressure of 1 *Pa* affects the general equation of flexural rigidity of the beam provided in Equation 4.25 [26]. The new flexural rigidity D_a becomes the expression shown in Equation 4.26.

$$D = \frac{Eb^3}{12 \cdot (1-\nu^2)} \tag{4.25}$$

$$D_a = \frac{(E+P) \cdot b^3}{12 \cdot (1-\nu^2)} \tag{4.26}$$

where P is the pressure, b is the beam thickness, E is the modulus of elasticity of the beam, and ν is the Poisson's ratio [25].

Solving the kinetic and potential energies for the deflection of the beam, assuming $\frac{\partial^2 \varphi}{\partial x^2} = \phi(x)$, results in having the energy equation shown in Equations 4.27 and 4.28.

$$PE = \frac{1}{2}\int_0^L D_a A_i^2 \phi_i^2 e^{2\omega t} dx \tag{4.27}$$

$$KE = \frac{1}{2}\int_0^L (m + m_a) \cdot A_i^2 \varphi_i^2 \cdot \omega_{wet}{}^2 \cdot e^{2\omega t} dx \tag{4.28}$$

where m_a is the script used for representing the added mass on the beam. By equating the kinetic and potential term represented in Equation 4.29 and defining a mass ratio as $M = \frac{m}{m_a}$, the expression for natural frequency is obtained as [25]:

$$\frac{A_i^2}{2}\int_0^L D_a \phi_i^2 e^{2\omega t} dx = \frac{A_i^2}{2}\omega_{wet}{}^2 \cdot m\int_0^L (1+M) \cdot \varphi_i^2 \cdot e^{2\omega t} dx \tag{4.29}$$

$$\omega_{wet}{}^2 = \frac{\int_0^L D_a \phi_i^2 e^{2\omega t} dx}{m\int_0^L (1+M) \cdot \varphi_i^2 \cdot e^{2\omega t} dx} \tag{4.30}$$

Assuming homogenous fluid medium, the flexural rigidity and mass ratio are independent of *x*, and they can be excluded from the integration. Moreover, the final expression for wet natural frequency, when the beam is immersed in water is provided in Equation 4.31.

$$\omega_{wet}{}^2 = \frac{LD_a \int_0^L \phi_i^2 e^{2\omega t} dx}{m \cdot (1+M)\int_0^L \varphi_i^2 \cdot e^{2\omega t} dx} = \frac{LD_a}{m \cdot (1+M)} \tag{4.31}$$

In the general case when there is not extra medium added to the beam, the same procedure is used in order to find its dry natural frequency in the case when the beam is placed in air/vacuum.

Similarly, the dry natural frequency is [25]:

$$\omega_{dry}{}^2 = \frac{LD}{m} \tag{4.32}$$

The frequency ratios defined earlier in Equations 4.6 and 4.7 are used along with Equations 4.31 and 4.32 in order to solve for the added mass term. The obtained added mass expression is described in Equation 4.33.

$$m_a = \frac{m \cdot D \cdot (R-1)}{D_a + D \cdot R} \tag{4.33}$$

The obtained natural frequencies represented earlier in Table 15 are used in Equation 4.33 provided above in order to calculate the added mass M_a for each mode shape i. The obtained added mass values are tabulated in Table 17 below. According to [24], the obtained values indicates that the added mass values of the lower modes are higher compared to the higher modes.

Table 17: Added Mass Values Through Beam Theory

Beam Theory for the MEMS	
Mode	Added Mass (g)
i	M_{ia}
1	4.974×10^{-31}
2	3.711×10^{-31}

4.1.5. Comparison. In this subsection, the added mass values calculated through acoustic method and beam theory are compared to each other as well as to the general added mass values. The general added mass value refers to the calculation of added mass using Equations 4.6 and 4.7. For the case of comparison, added mass values obtained through the acoustic method and the beam theory are tabulated in Table 18 below, and the percentage difference for both modes is calculated.

Table 18: Added Mass Obtained from Acoustic Method vs. Beam Theory

Added Mass			
Mode	Acoustic Method	Beam Theory	Difference
i	M_{ia}(g)	M_{ia}(g)	*(%)*
1	2.538×10^{-31}	4.974×10^{-31}	48.5
2	2.072×10^{-31}	3.711×10^{-31}	44.2

The percentage difference between the obtained added mass values of the acoustic method and beam theory is calculated and tabulated above for each mode.

The first mode added mass values are about 48.5% different, which is relatively high and represents the deviation of the process calculation. As it is mentioned earlier, the process calculations are deviating because the acoustic method mainly uses the natural frequencies of wet and dry cases in order to evaluate the added mass values. On the other hand, the beam theory considers the properties of the beam; for example, Young's modulus of elasticity, Poisson's ratio, moment of inertia as well as the wet and dry natural frequencies. These additional details make the added mass calculation more inclusive of involved parameters. Similarly, this will affect the percentage difference between the obtained added mass values of these two methods for the second mode of vibration. The second mode percentage difference is about 44.2% which is slightly lower than the first mode, yet the difference is considered high.
Furthermore, the added mass values obtained from both methods are compared to the general added mass values. Table 19 represents the tabulated data of the acoustic theory versus general method for the mean of contrast in order to check the reliability of the suggested method.

Table 19: Added Mass Obtained from Acoustic Method vs. General Method

Added Mass			
Mode	Acoustic Method	General Method	Difference
i	M_{ia}(g)	M_{ia}(g)	*(%)*
1	2.538×10^{-31}	3.610×10^{-31}	29.6
2	2.072×10^{-31}	2.834×10^{-31}	26.8

The obtained percentage difference for the first mode is about 29.6 %, which indicates that the added mass value obtained from acoustic method is deviating from the added mass value obtained from general method by less than 30%. This difference is slightly lower for the second mode of vibration with 26.8% deviation. The main reason behind this percentage difference is the variation in defining the frequency ratio than that of the general method. The percentage in the second mode is lower since the added mass values are smaller in the higher modes.

Similarly, the added mass values obtained from beam theory are represented against the general added mass values which are provided in Table 20 in order to check the reliability of the suggested method.

Table 20: Added Mass Obtained from Beam Theory vs. General Method

Added Mass			
Mode	Beam Theory	General Method	Difference
i	M_{ia} (g)	M_{ia} (g)	*(%)*
1	4.974×10^{-31}	3.610×10^{-31}	27.4
2	3.711×10^{-31}	2.834×10^{-31}	23.6

The percentage differences between the general method and the beam theory are tabulated in Table 20 above. The percentage difference of the first mode is found to be 27.4%, which points out that the added mass value calculated through beam theory and the added mass value obtained using general method are deviating by less than 30%. The second mode percentage difference is calculated to be 23.6% which is lower than the first mode of vibration. The deviation between these two methods is mainly due to the difference in the characteristics of the equations. The added mass equation obtained from the beam theory is inclusive of both natural frequencies and beam internal properties, such as density, Young's modulus of elasticity and Poisson's ratio. In other words, the beam theory is dependent on the material type of the beam as well as the wet and dry natural frequencies. Comparison of the percentage differences tabulated in the Tables 19 and 20 reveals that the beam theory is considerably closer to the general method compared to the acoustic method. Therefore, added mass calculations through the beam theory would result in a more accurate result.

Chapter 5. Added Mass Formulation

5.1. Formulation

The obtained formula for the added mass effect of this specific MEMS is represented in terms of few parameters involved in the process. In other words, the formula is a function of parameters such as linear spring stiffness, torsional spring stiffness, dry natural frequency, wet natural frequency, MEMS' dimensions and fluid density; these parameters will be explained in details later in the text. In addition to the above parameters, added mass would also have an extra part which is a mass due to displaced water close to the MEMS.

The proposed formula includes a correction factor for flexural modes Γ_f since the flexural modes are extensively affected by immersion in fluid. This correction factor is taken from Eysden et al. [27] work and it is represented in Equation 5.1 below.

$$\Gamma_f = \frac{1+0.74273\kappa+0.14862\kappa^2}{1+0.74273\kappa+0.35004\kappa^2+0.058364\kappa^3} \tag{5.1}$$

In the above equation, the κ is the wave number defined as a fraction of frequency *f* over the speed of sound *c* provided in Equation 5.2.

$$\kappa = \frac{f}{c} \tag{5.2}$$

The general equations of natural frequencies for wet and dry cases are represented in the Equations 5.3 and 5.4.

$$\omega_{wet} = \sqrt{\frac{K_{eq}}{(m_s + m_a \cdot \Gamma_f)}} \tag{5.3}$$

$$\omega_{dry} = \sqrt{\frac{K_{eq}}{m_s}} \tag{5.4}$$

In the above equations, K_{eq} is representing the equivalent of linear and torsional stiffness in the system. m_s and m_a are masses corresponding to the structure and the amount of fluid loading, respectively. It is important to note that the mss of structure is as shown in Equation 5.5.

$$m_S = \rho_{Al} \cdot t \cdot b \cdot L \tag{5.5}$$

The equivalent stiffness is obtained based on the Potential Energy method. Due to symmetry of this specific MEMS, the equivalent stiffness is shown in Equation 5.6 in which K_1 represents the linear spring and K represents the torsional spring.

$$K_{eq} = K_1 L^2 + K \tag{5.6}$$

Inserting Equation 5.4 into Equation 5.3, and solving for added mass term m_a results in the Equation 5.7 provided below. The term *i*, as stated earlier, is the notation for the mode number.

$$m_a = K_{eq} * \left(\frac{1}{\omega_{iWet}^2 \Gamma_f} - \frac{1}{\omega_{iDry}^2 \Gamma_f} \right) + m_{disp} \tag{5.7}$$

In the above equation displaced mass of water is represented as m_{disp} which is equal to the volume of the MEMS multiplied by the fluid density of water. This expression is shown in Equation 5.8.

$$m_{disp} = \rho_f \cdot t \cdot b \cdot L \tag{5.8}$$

By substituting Equations 5.8 and 5.6 into Equation 5.7, the final formula proposed for the added mass for the fluid structure interactions on this specific MEMS for different modes is obtained and shown in Equation 5.9. It is important to state that in this study, only the first two modes are considered.

$$m_a = \left[K_1 L^2 + K \right] * \left(\frac{1}{\omega_{iWet}^2 \Gamma_f} - \frac{1}{\omega_{iDry}^2 \Gamma_f} \right) + \rho_f \cdot t \cdot b \cdot L \tag{5.9}$$

5.2. Calculations

In order to calculate the arithmetic value for the added mass, according to the established formula, the numerical values of the involved parameters will be used. These baseline parameters for this specific MEMS have been defined earlier in Table 14. Moreover, the natural frequencies were obtained using the COMSOL *multiphysics 4.4* and provided two modes for both wet and dry cases earlier in Table 15.

Meanwhile, the correction factor is a parameter which requires an independent calculation before it can be applied to the Equation 5.9.

To calculate the correction factor Γ_f, the wave number κ should be intended first. Doing so, the average frequency range and the speed of sound in water are implemented in Equation 5.2. The obtained values for correction factor Γ_f, and wave number κ are shown in the Table 21.

Table 21: Correction Factor Calculated Value

Symbol	Numerical Value
κ	$0.14\ {}^{1}\!/_{m}$
Γ_f	$0.99\,m^2$

Implementation of the wave number κ, as it is defined in the table above, results in a correction factor which is approximately equal to unity. This approximated value will be used in the calculation process of the added mass. Consequently, the numerical value of the added mass based on Equation 5.9 is calculated. The values for the first two modes are provided in Table 22.

Table 22: Added Mass Values Through Proposed Established Formulation

Proposed Added Mass Formula for the MEMS	
Mode	Added Mass (g)
i	M_{ia}
1	5.391×10^{-31}
2	3.036×10^{-31}

These obtained values, as expected, shows that the added mass effect gets smaller as the mode number increase.

5.3. Comparison

In this section, the calculated values will be validated through comparison with the well known methods. These methods have been studied earlier in this report and the added mass values for the first two modes were tabulated. The methods used are

Acoustic method and Beam theory in which the obtained added mass values were tabulated in Table 16 and Table 17, respectively.

Firstly, the added mass values are provided in comparison with the general method of calculating the added mass which was discussed in Equations 4.6 and 4.7. Table 23 represents the tabulated data of the proposed formula versus general method for the mean of contrast in order to check the reliability of the suggested formulation.

Table 23: Added Mass Obtained from Proposed Formulation vs. General Method

Added Mass			
Mode	Proposed Formulation	General Method	Difference
i	M_{ia}(g)	M_{ia}(g)	*(%)*
1	5.931×10^{-31}	4.974×10^{-31}	16.1
2	3.036×10^{-31}	3.711×10^{-31}	18.2

The percentage differences between the obtained added mass values of the proposed formula and the general method are calculated and tabulated above for each mode. The obtained average difference is about 17.2% which indicates that the obtained values are not far from each other. This difference is mainly due to use of extra detail in the anticipated formula, such as correction factor, fluid's density and mass of displaced water around the MEMS.

Secondly, the added mass values are provided in comparison with the Acoustics method of calculating added mass. Table 24 represents the tabulated data of the proposed formulation versus Acoustics method for the sake of contrast in order to check the reliability of the formula.

Table 24: Added Mass Obtained from Proposed Formulation vs. Acoustics Method

Added Mass			
Mode	Proposed Formulation	Acoustic Method	Difference
i	M_{ia}(g)	M_{ia}(g)	*(%)*
1	5.931×10^{-31}	2.538×10^{-31}	57.2
2	3.036×10^{-31}	2.072×10^{-31}	31.7

The percentage differences between the obtained added mass values of the proposed formulation and acoustic method are calculated and tabulated above for each mode. In the first two modes, the added mass values are about an average of 44.5% different, which is relatively high and represents the deviation of the process calculation. As mentioned earlier, the process calculations are deviating because the acoustic method mainly uses the natural frequencies of wet and dry cases in order to evaluate the added mass values. On the other hand, the suggested formula is mainly uses the MEMS parameters' extensively.

Lastly, the added mass values are provided in comparison with the beam theory for the calculation of added mass values. Table 25 represents the tabulated data of the proposed formulation versus beam theory for the sake of contrast in order to check the reliability of the suggested formula.

Table 25: Added Mass Obtained from Proposed Formulation vs. Beam Theory

Added Mass			
Mode	Proposed Formulation	Beam Theory	Difference
i	M_{ia}(g)	M_{ia}(g)	*(%)*
1	5.931×10^{-31}	4.974×10^{-31}	16.1
2	3.036×10^{-31}	3.711×10^{-31}	22.2

The percentage differences between the obtained added mass values of the proposed formulation and beam theory are calculated and tabulated above for each mode. The average percentage difference of 19.2% shows that these two method of the added mass calculations are relatively close. The calculated values are not deviating since there are many common involved parameters in both methods. The beam theory considers the properties of the beam; for example, Young's modulus of elasticity, Poisson's ratio, moment of inertia as well as the wet and dry natural frequencies. These mentioned and few additional parameters have been also implemented onto the proposed formula.

As mentioned earlier in the deriving process, the proposed formulation nature is based on the both acoustics and beam theory. According to the obtained data, the formula is much closer to the beam theory than Acoustics method. The comparison

between the mentioned methods have shown that the proposed formula is reasonable and valid. However, the main validation process would require an experimental instrumentation with the specific MEMS. The experimental setup is considered as a future work and it was not possible to be done due to the lack of available fund. Nevertheless, the experimental setup and its required facilities has been defined in the conclusion section.

5.4. Validation

5.4.1. Cantilever Beam. In this section, the proposed formula is going to be evaluated for the popular case of the cantilever beam. This process is the validation of the formula according to the literature other than experimental. Consequently, a simulation in an acoustic module is done with a cantilever beam with the same dimension as one side of the MEMS studied. The dimensions are as follows: width of $1\times10^{-6}m$, length of $1\times10^{-6}m$ and thickness of $0.05\times10^{-6}m$. The material used is same as the MEMS which is Aluminum H3003-18. The same identical conditions are applied for this cantilever beam. The obtained natural frequencies for the case of wet and dry for first two modes are tabulated in Table 26.

Table 26: Eigenmode Numbers and Corresponding Natural Frequencies

Cantilever Beam		
Mode	Natural Frequency in air	Natural Frequency in water
i	$\omega_i Dry$ (Hz)	$\omega_i Wet$ (Hz)
1	71.2	57.1
2	101.5	81.2

Then the stiffness of the cantilever beam is obtained through the Equation 5.10 shown below.

$$K = \frac{3EI}{L^3} \tag{5.10}$$

Having all the requirements, the calculation is done using the proposed formulation Equation 5.9 mentioned earlier in this chapter. This equation does have a small modification in which the equivalent stiffness does not include any torsional stiffness. The modified equation of the proposed formula is provided in Equation 5.11.

$$m_a = \left[K_1 L^2 \right] * \left(\frac{1}{\omega_{iWet}{}^2 \Gamma_f} - \frac{1}{\omega_{iDry}{}^2 \Gamma_f} \right) + \rho_f \cdot t \cdot b \cdot L \qquad (5.11)$$

The added mass values for the first two modes are tabulated in Table 27 shown below.

Table 27: Added Mass Values Through Proposed Established Formulation

Proposed Added Mass Formula for the Cantilever Beam	
Mode	Added Mass (g)
i	M_{ia}
1	1.43×10^{-31}
2	0.056×10^{-31}

The validation is done with the comparison of the analytical added mass formulation, mentioned in the chapter 3, versus the proposed formula to see whether the formula is valid for this popular case or not. The analytical added mass formulation is provided in Equations 3.7 - 3.12. The result of comparison is tabulated in Table 28 represented below.

Table 28: Added Mass Obtained from Proposed Formulation vs. Analytical Formulation for Cantilever Beam

Added Mass for Cantilever Beam			
Mode	Proposed Formulation	Analytical Formulation	Difference
i	M_{ia}(g)	M_{ia}(g)	*(%)*
1	1.43×10^{-31}	1.50×10^{-31}	4.67
2	0.056×10^{-31}	0.06×10^{-31}	6.75

As it is shown in the Table 28 above, the average percentage differences between the analytical calculation of added mass and the proposed formulation are less than 10% for each case. This low difference can show that the established formulation is a valid formula for calculating the added mass value for the structures in micro dimension. However, the validation through experimentation is a mandatory process which needs to be done in future works.

5.4.2. Displaced Mass. In this section, further analysis is done to see the effect of displaced mass (m_{disp}) on the added mass value. First of all, the added mass to the air must be obtained using the proposed formulation. In this analysis, the popular case of cantilever beam with the exact same dimensions as defined in section 5.4.1 is used. Moreover, the pressure acoustics module is used to find the first two modes of natural frequencies when the cantilever beam is placed in vacuum. The obtained natural frequencies for the first two modes, coupled with air and vacuum, are tabulated in Table 29. Where $\omega_i Vac$ is the natural frequency of the beam in the vacuum, and $\omega_i air$ is the natural frequency of the beam interacting with air.

Table 29: Eigenmode Numbers and Corresponding Natural Frequencies

Cantilever Beam		
Mode	Natural Frequency in vacuum	Natural Frequency in air
i	$\omega_i Vac$ (Hz)	$\omega_i air$ (Hz)
1	71.2	71.2
2	101.7	101.5

The obtained natural frequencies are implemented in the proposed formulation provided in Equation 5.11. When the cantilever beam is coupled with air, its natural frequencies slightly drops compared to the natural frequencies in the case of vacuum. More specifically, the coupling behavior of the cantilever beam can also be interpreted in terms of added mass. Therefore, the added mass values due to air, for each mode, are tabulated in Table 30.

Table 30: Added Mass Values Through Proposed Established Formulation

Proposed Added Mass Formula for the Cantilever Beam	
Mode	Added Mass (g)
i	M_{ia}
1	0.062×10^{-31}
2	0.15×10^{-31}

The added mass value for the first mode is not a zero value even though the natural frequencies in both vacuum and air mediums are the same. The added mass value for the first mode equals to a small value which is mainly due to the perturbation made by the beam's vibration in the air. However, this value is small in amount compared to the mass of the cantilever beam, but the added mass effect on the structure remains. The comparison between the structural mass M_s and the added mass in the scale of 10 is provided in Table 31. The added mass effect can be ignored when the surrounding medium have zero density. Typically, added mass effect is neglected when the structure is placed in vacuum and no coupling is happening between mediums.

Table 31: Structural Mass and Added Mass Comparison

Cantilever Beam		
Mass	Mass Values (g)	Difference (%)
M_s	1.365×10^{-31}	45
M_a	0.062×10^{-31}	

Chapter 6. Conclusion

This work aimed at demonstrating how variations of geometries' parameters would affect the fluid loading effect in water through parametric investigation for common geometry shapes. More specifically, this research introduced an added mass effect study for fluid structure interaction while a specific MEMS is submerged in water medium. Subsequently, based on the mentioned studies, an added mass formulation is derived for this specific beam based MEMS. The parametric investigation study is conducted numerically to demonstrate the variation of geometries' parameters and the corresponding behavior of the fluid loading effect in water using COMSOL *Multiphysics 4.4*. The added mass values of the structures obtained from both acoustic domain analysis and fluid domain analysis are compared to each other as well to the analytical values. These calculated results of added mass of the common geometry shapes are in accordance with the analytical calculations and the discrepancy behavior of added mass amount due to the establishment of variation of geometries' parameters for the common geometry shapes. For the rectangular cantilever beam, it is found that the increase in length and cross section results in the increase of added mass value. In the case of sphere, the obtained result shows the relation in which increasing the added mass value happens as the radius increases. Finally, the parametric study on the circular cylinder reveals that as either the radius or length increases the added mass gets higher. The analytical formulas suggested by White [12] works out the best for the circular cylinder and sphere, yet the natural frequency based formula recommended by Chu [13] works the best for rectangular cantilever beam.

Although the main objective of this study was to compute the hydrodynamic mass of common geometry shapes, e.g., rectangular cantilever beam, solid sphere and circular cylinder, is extended to determining the computed added mass with the variation of geometric parameters so that such correlations may be used for design purposes. The parametric study have enhanced knowledge of added mass phenomenon in which it built the basis for added mass study conducted in this research. A specific beam based MEMS was selected for this study. The selected system is one of the most popular MEMS available in the industry, and the studies of this system are increasing gradually. The added mass study for this MEMS revealed

how fluid loading on this structure could affect its performance, mainly in terms of natural frequencies. The natural frequencies for the first two modes are analyzed for two different cases, when the MEMS is placed in air and when it is submerged in water. Analyzing these two cases has exposed the fluid loading effect in terms of 80% drop in natural frequencies when MEMS was submerged in water compared to the case where the MEMS was in contact with the air. This natural frequency drop is mainly due to the fluid loading effect and it has been interpreted by the means of added mass. It is revealed that the added mass effect is greater at lower modes of vibration and this effect gets smaller at higher modes. The added mass study for the specific MEMS is done and compared through two different method; the acoustic method and beam theory. Studies show that the beam theory provides considerably closer added mass values to the general added mass method. The added mass formulation for this specific MEMS is obtained based on the beam theory and Acoustic method. The numerical values of the proposed formulation are compared with all three method; general method, Acoustic theory and Beam theory. The comparison revealed that the calculated added mass values are considerably closer to the general method and Beam theory method, respectively.

As stated earlier, submerged structure experiences the effect of added fluid on its behavior. One of the most important fluid effects on structure is the added damping coefficient C_a. This additional damping term is mainly a hydrodynamic damping since water density and its forces are considerably higher compared to the case of unavailability of water [28]. In his PhD dissertation, Venugopal [28] mainly studied the damping due to water effect for a submerged cylinder, yet he mentions the general idea for all the available types of structures. He stated that the fluid damping is dependent on several parameters; for instance, density of fluid, kinematic viscosity, shape of cross section, length, mass, amplitude of displacement and surface roughness of the structure [28]. He specified an additional case when the added fluid is in stationary mode. More specifically, it is noted that damping due to motion of structure in stationary water is mainly dependent on the Reynolds number in terms of the velocity of the structure and the amplitude of the response [28]. As a structure moves in fluid, the imposing forces of fluid slow down the movement of the structure. These forces are called drag forces, representing the combination of pressure drag and friction drag [29]. Pressure drag is the force imposed on the structure; whereas,

friction drag is the shear stress at the wall of the fluid container [29]. According to Fossen's findings in his book [30], when a structure or body is submerged in water and it is forced to oscillate due to harmonic frequency based wave, the damping effect of water is called linear frequency dependent potential damping. The drag coefficient is not a constant value, and it is dependent on several parameters, such as flow condition and shape of the structure; more specifically, it is the function of Reynolds number which clarifies the flow condition [30]. Consideration of the damping due to water while studying the fluid loading effect on MEMS could be an interesting area to investigate in further research.

It is highly recommended to validate the obtained added mass formula through experimentation. An experimental configuration based on the available equipment in the previous experiments is suggested. This experimentation could not be done due to funding and time constraints prior to this project. The main goal of this experiment is to detect the first and second natural frequencies of the proposed vibrating structure in both water and air mediums. One of the main required equipments for this experiment is the LDV which is a scientific device used for detecting non-contact surface vibration measurements. This non-contact measuring device detects the structural response of a structure undergoing the test, such as damping, natural frequency and mode shapes. Sriram et al. [31] states that these scanning LDVs are not accurate for a submerged vibrating structure since the spread signal arrives in discontinuous bursts analogous to the particles crossing the LDV's probe volume which may cause error in measurements. To solve the inaccuracy issue, it is recommended to use a calibrator before considering the final measurements. Accordingly, it is suggested to use a handheld calibrator as the objective prior to the actual measurement and then execute the measurement with a turned on calibrator. It is also recommended to execute these measurements in time domain, so that if there is any noise added to signal, it can be detected and removed accordingly. If this medium validation measurement is executed with the estimated result, it can be stated that the medium (water) does not interfere with the consequent actual measurements [32]. The equipment needed for this validation experiment is a shaker that can be used in both mediums to vibrate the structure. For this purpose, an electromagnetic or a hydraulic shaker can be used at the point of interest of structure [33]. For running the experiment, the electromagnetic shaker has to be connected to an output gate of a FRA with a certain voltage. This

FRA will transform the voltage into a magnetic harmonic force of the same frequency range [34]. The shaker will excite the structure by the harmonic force at a certain frequency, and data for force, response signal, and the phase information will be recorded [33]. Another main factor that should be considered for the experimentation is the design of the water container. It is recommended to select a relatively large container, so that the walls would not have a significant effect on the experimental result [35]. Considering all the factors mentioned earlier, the proposed experimental setup is where the structure is placed on the electromagnetic shaker. The magnetic shaker is connected to the output of FRA system for signal generation and hence its transformation to mechanical force. This connection could be done using either smart tether wires, which are mainly designed for underwater use only, or through a wireless FRA system [36]. The excitation of the structure will be scanned using a LDV system. However, the LDV system is only calibrated for air measurements, so presence of water will lead to a diffraction of laser beams. To overcome this problem, the following proposed method can be used. This method involves a LDV for acousto-optic sensing in which the system detects the propagated data from vibrating water-air interfacing surface [37], where acousto-optic is a division of physics which focuses on the study of interaction between sound waves and light waves. On the other hand, the optical diffraction index of water can be considered for eliminating the inaccuracies due to laser vibrometer [38]. The LDV system is connected to a DAQ which is an interference between the signal and a computer to convert the analog signals of the sensor into digital values. According to the literature, when running the experiment for the case of submerged, a handheld calibrator is added in between the LDV and DAQ. This experiment will allow the user to obtain the first and second natural frequencies of vibrating structure in both mediums. Then, these values will be used for calculation of experimental added mass and comparison with the obtained analytical values.

References

[1] S. M. Firdaus and H. Omar and I. A. Azid, "High Sensitive Piezoresistive Cantilever MEMS Based Sensor by Introducing Stress Concentration Region (SCR)," in Finite Element Analysis - New Trends and Developments, *Open Science InTech*, 2012, pp. 225-229.

[2] D. R. Brumley, "*The Dynamics of High Frequency NanoElectroMechanical Resonators in Fluid*," .Sc Thesis, University of Melbourne, Melbourne, Australia,2008.

[3] W. Mai, "Home Page - Professor Zhong L. Wang's Nano Research Group," June, 2002. [Online]. Available: http://www.nanoscience.gatech.edu/zalwang/research/afm.html. [Accessed: May. 15, 2016]

[4] J. E. Sader and C. A. Van Eysden, "Frequency Response of Cantilever Beams Immersed in Compressible Fluids with Applications to the Atomic Force Microscope," *Applied Physics*, vol. 84, no. 1, pp. 1-8, July. 1998.

[5] F. Liu and H. Li and H. Qin and B. Liang, "Added Mass Matrix Estimation of Beams Partially Immersed in Water using Measured Dynamic Response," *Sound and Vibration*, vol. 333, no. 20, pp. 5004-50017, Sept. 2014.

[6] P. Causin and J.F. Gerebau and F. Nobile, "Added-Mass Effect in the Design of Partitioned Algorithms for Fluid-Structure Problem," Computer *Methods in Applied Mechanics and Engineering*, vol. 194, pp. 4506-4527, Dec. 2004.

[7] R. K. Singhal and W. Guan and K. Williams, "Modal Analysis of a Thick-Walled Circular Cylinder," *Mechanical System and Signal Processing*, vol. 16, no.1, pp.141-153, Jan. 2002.

[8] E. Da Lozzo and F. Auricchio and G. M. Calvi, "Added Mass Model for Vertical Circular Cylinder Immersed in Water," in *Proceedings of the 15th World Conference on Earthquake Engineering*, 15WCEE, 24-28 Sept. 2012, Lisbon, Portugal, pp. 1-10.

[9] R. N. Govardhan and C. K. Williamson, "Vortex-Induced Vibrations of Sphere," Journal *of Fluid Mechanics*, vol. 531, pp. 11-47, May. 2005.

[10] S. A. Fackrell, "*Study of the Added Mass of Cylinders and Spheres*," Ph.D. dissertation, University of Windsor, Ontario, CA, Canada, 2011.

[11] H. Ghassemi and E. Yari, "The Added Mass Coefficient Computation of Sphere, Ellipsoid and Marine Propellers using Boundary Element Method," *Polish Maritime Research*, vol. 18, no. 68, pp. 17-26, 2011.

[12] F. M. White, "Potential Flow and Computational Fluid," in *Fluid Mechanics*, 5th ed. New York: McGraw-Hill, 2003, pp. 566-568.

[13] W. H. Chu, "Further Developments of a More Accurate Method for Calculating Body-Water Impact Pressure" in *Fundamental Hydrodynamics Research Program*, Tech. Rep. no. 2, pp.10-52, April. 1963.

[14] M. Elgabaili, "*Hydrodynamic Mass of Bluff Bodies with and without Cavity*," M. S. thesis, California State University, Northridge, California, 2012.

[15] J. C. Jo, "Fluid Structure Interactions," in *Pressure Vessels and Piping Systems - Encyclopedia of Life Support Systems*, Tech. Rep. no. 5, pp. 11-45, Sept. 2010.

[16] K. Vikestad and C. M. Larsen and J. K. Vandiver, "Damping of Vortex- Induced Vibrations," in *Proceedings of the Offshore Technology Conference*, OTC 11998, 1-4 May. 2000, Texas, United State of America, pp. 1-7.

[17] D. Sedlar and Z. Lozina and D. Vucina, "Experimental Investigation of the Added Mass of the Cantilever Beam Partially Submerged in Water," *Technical Gazette*, vol. 18, no. 4, pp. 589-594, April. 2011.

[18] S. Mönkölä, "Numerical Simulation of Fluid-Structure Interaction Between Acoustics and ElasticWaves," *Studies in Computing Fluid Structure Interaction*, vol. 36, pp. 1-129, 2011.

[19] Q. Liang, C. Rodríguez, E. Egusquiza, X. Escaler, M. Farhat, and F. Avellan, "Numerical simulation of fluid added mass effect," *Computers & Fluids*, pp. 1106-1118, 2010.

[20] L. E. Kinsler and A. R. Frey, *Fundamentals of Acoustics*, 2d Ed. New York: Wiley, 1962.

[21] O. C. Zienkiewicz and R. E. Newton, "Coupled Vibrations of a Structure Submerged in a Compressible Fluid," *Symposium on Finite Element Techniques*, 1969.

[22] C. C. Liang, C. C. Liao, Y. S. Tai, and W. H. Lai, "The Free Vibration Analysis of Submerged Cantilever Plates," *Ocean Engineering*, vol. 28, no. 9, pp. 1225 - 1245, Sept. 2001.

[23] L. Meirovitch, *Elements of Vibration Analysis*, 2nd Ed. New York: McGraw-Hill, 1986.

[24] R. Shabani, H. Hatami, F. G. Golzar, S. Tariverdilo, and G. Rezazadeh," Coupled Vibration of a Cantilever Micro-Beam Submerged in a Bounded Incompressible Fluid Domain," *Acta Mechanica Acta Mech*, pp. 841-850, 2012.

[25] D. Lin and B. T. Yakub, "Interface Engineering of Capacitive Micromachined Ultrasonic transducer for medical applications," *IEE Symposium on Ultrasonics*, vol. 20, no. 1, pp. 8-31, 2011.

[26] R. Gruter, "*Simultaneous Detection of Added Mass and Change in Stiffness using Micromechanical resonator,"* M.S. thesis, University of Basel, Basel, CH, Switzerland, 2009.

[27] C.V. Eysden and J. E. Sader, "Resonant Frequencies of a Rectangular Cantilever Beam Immersed in a Fluid," *J. Appl. Phys. Journal of Applied Physics*, vol.100, no. 11, p. 114916, 2006.

[28] M. Venugopal, "*Damping and Response Prediction of a Flexible Cylinder in a Current* ," Ph.D. dissertation, Massachusetts Institute of Technology, Massachusett, United State of America, 1996.

[29] A. Bakker, "Reynolds Number and Drag on Immersed Bodies," *Applied Computational Fluid Dynamics*, vol.1, no. 2, pp.1- 4, 2011.

[30] T. H. Fossen, "Maneuvering Theory," in *Handbook of Marine Craft Hydrodynamics and Motion Control*, Wiley, 2011, pp.122-126.

[31] P. Sriram and S. Hanagud and J. I. Craig, "Modal Analysis," *The International Journal of Analytical and Experimental Modal Analysis*, vol.7, no. 3, pp. 169-178, July. 1992.

[32] K. B. Gatzwiller and K. B. Ginn and A. Betts and S. Morel, "Practical Aspects of Successful Laser Doppler Vibrometry based Measurements," in *Proceedings of the Society for Experimental Mechanics Conference*, IMAC-XXI, 2003, pp. 1-6.

[33] K. Cheng, Machining Dynamics Fundamentals, Applications and Practice: *Dynamic Analysis and Control*, Middlesex: Springer, 2009, pp. 43-46.

[34] C. T. F. Ross, Pressure Vessels External Pressure Technology: *Vibration of a thin-walled shell under external water pressure using ANSYS*, 2nd ed. Cambridge: Woodhead, 2011, pp. 394-396.

[35] J. Singer and J. Arbocz and T. Weller, Buckling Experiment:Experimental Methods in Buckling of Thin-Walled Structure: *Stiffened Shells*, 2nd ed. Canada:John Wiley & sons, Inc, 2002, pp. 1019-1021.

[36] A. Zoksimovski and D. Sexton and M. Stojanovic and C. Rappaport," Underwater Electromagnetic Communications Using Conduction - Channel Characterization," in *Proceedings of the ACM International Conference on Underwater Networks & systems*, WUWNet'12, 5-6 Nov. 2012, Los Angeles, CA, United State of America, pp.1-7.

[37] J. M. Buick and J. A. Cosgrove and P. A. Douissard and C. A. Greated and B. Gilabert, "Application of Acousto-optic Effect to Pressure Measurements in Ultrasound Fields in Water using a Laser Vibrometer," *Review of Scientific Instruments*, vol. 75, no. 10, pp.3-5, Sept. 2004.

[38] T. F. Argo and P. S. Wilson and V. Palan, "Measurement of the Resonant Frequency of Single Bubbles using a Laser Doppler Vibormeter," *Journal of Acoustical Society of America*, vol. 123 , no. 6, pp. 2-5, June. 2008.

Appendix A

The Matlab codes which has been used for studying the vibrational behavior of the MEMS without any fluid medium is provided below. Where analytical and transfer function's natural frequencies were compared.

```
clc
clear all
close all
%% Forced-Damped Vibration for two Coupling Beams connected through torsional
%% Spring
%% Harmonic input force e^iwt
L=1e-6;
m1=1.365e-31;
m2=1.365e-31;
k1=20e-6;
k2=20 e-6;
k=1000 e-6;
c1=0;
c2=0;
w=20;     %w=2*pi*f frequency

%% Mass, Stiffness, Damping Matrices

M=[m1 0; 0 m2];
C=[-c1*L-c2*L c2*L; c2*L -c2*L];
K=[k*L-k1*L+k2*L k2*L-k*L; k2*L-k*L k*L-k2*L];

%% Physical matrix of 2DOF system
%% analytical natural Frequencies

a=((w*c1)+(w*c2));
b=((-w*w*m1)+k-k1+k2);
```

```
d=(k2-k);
f=((-w*w*m2)+k-k2);
h=(w*c2);

A=[a b -h d; b -a d h; -h d h f; d h f -h];

[V,D]=eig(A);
freq=sqrt(D);

W1anal=freq(3,3)
W2anal=freq(4,4)

%% Natural Frequencies form Response plot
%% Numerator for TF#1
a0= m2;
a1=(w*i*m2-c2);
a2=(k-k2-((w*i)*c2));
a3=w*i*(k-k2);
num1=[a0 a1 a2 a3];

%% Numerator for TF#2
a00=m1;
a11=(-c1-c2+(w*i*m1));
a22=(k-k1+k2-((w*i)*c2)-((w*i)*c1));
a33=w*i*(k-k1+k2);
num2=[a00 a11 a22 a33];

%% Denominator
T=m1*m2;
N=((-m1*c2)-(m2*c1)-(m2*c2));
P=((k*m1)-(k2*m1)+(c1*c2)-(k1*m2)+(k*m2)+(k2*m2)+1);
Q=((-k*c1)+(k2*c1)+(k1*c2)-(2*k2*c2));
R=((2*k*k2)-(k*k1)+(k1*k2)-(2*k2*k2));
```

```
b0=T;
b1=N;
b2=(P+(T*w*w));
b3=(Q+(2*w*w*N));
b4=(R+(2*w*w*P)+(T*(w^4)));
b5=((2*w*w*Q)+((w^4)*N));
b6=((2*w*w*R)+((w^4)*P));
b7=((w^4)*Q);
b8=(R*(w^4));

denum=[b0 b1 b2 b3 b4 b5 b6 b7 b8];
sys1= tf(num1,denum);
sys2=tf(num2,denum);

%% Frequency Plot
wf= logspace(-1,3,1000000);
Y=freqresp(num1,denum,wf);
y1=abs(Y);
y2=angle(Y);

subplot(2,1,1)
semilogx(wf,20*log10(y1));
grid on
ylabel('Magnitude (dB)')
title('Bode Diagram')

subplot(2,1,2)
semilogx(wf,y2*(180/pi));
grid on
ylabel('Phase (deg))')
xlabel('Frequency (Hz)')
%% Extracting Frequency from Bode plot
```

```
[Wn] =damp(sys2);

W1=Wn(3,1)
W2=Wn(7,1)

%% Difference Between Frequencies
Difference_W1= abs(((W1-W1anal)/W1)*100)
Difference_W2= abs(((W2-W2anal)/W2)*100)
```

Appendix B

The Matlab codes which has been used for symbolic study of wet and dry for the first two natural frequencies. The relationship between dry and wet frequencies are obtained using ratio.

```
clc
clear all
close all

syms w c m k k1 ma

%% Physical matrix of 2DOF sys
A=[(w*c)+(w*c) ((-w*w*m)+k-k1+k1) (-w*c) (k1-k); ((-w*w*m)+k-k1+k1) (-
w*c)+(-w*c) (k1-k) (w*c);-(w*c) (k1-k) (w*c) ((-w*w*m)+k-k1);(k1-k) (w*c) ((-
w*w*m)+k-k1) (-w*c)];
[V,D]=eig(A);
freq=sqrt(D);
W1dry=freq(3,3)
W2dry=freq(4,4)

%%Physical Matrix of 2DOF with Added mass
B=[(w*c)+(w*c) ((-w*w*(m+ma))+k-k1+k1) (-w*c) (k1-k); ((-w*w*(m+ma))+k-
k1+k1) (-w*c)+(-w*c) (k1-k) (w*c);-(w*c) (k1-k) (w*c) ((-w*w*(m+ma))+k-k1);(k1-
k) (w*c) ((-w*w*(m+ma))+k-k1) (-w*c)];
[S,N]=eig(B);
freqq=sqrt(N);
W1wet=freqq(3,3)
W2wet=freqq(4,4)

R1=W1wet/W1dry
R2=W2wet/W2dry
```

Vita

Afsoun Koushesh was born in 1991, in Shiraz, Iran. She moved to Tehran, Iran at the age of seven and continued her elementary school there. In 1999 she moved to Dubai, United Arab Emirates. She finished high school and directly joined the American University of Sharjah (AUS) to pursue her study Bachelor of Science in Mechanical Engineering. Right after she graduated in 2013, she received a graduate teaching assistance scholarship from the AUS to join the Mechanical Engineering Master program.